GEORGIA INSTITUTE OF TECHNOLOGY — OFFICE OF CONTRACT ADMINISTRATION

PROJECT ADMINISTRATION DATA SHEET

[x] ORIGINAL [ ] REVISION NO. _____

Project No. A-3383 GTRI/~~GIT~~ DATE 10/22/82

Project Director: E. F. Greneker MISC ~~School~~/Lab RAIL-IMD

Sponsor: Deutsche Forschungs-und Versuchsanstalt

4333 Per Rev. #1

Type Agreement: Agreement No. 55312-4337-82

Award Period: From 10/12/82 To 10/11/85 (Performance) _____ (Reports)

Sponsor Amount: Total Estimated: $ 48,352* Funded: $ 48,352

Cost Sharing Amount: $ None Cost Sharing No: _____

Title: Technical Consulting During Development of an Instrument Coherent Polarization Diversity Meteorological Radar

ADMINISTRATIVE DATA

OCA Contact William F. Brown x-4820

1) Sponsor Technical Contact:

Dr. Peter Meischner
Deutsche Forschungs-und Versuchsanstalt
fur Physik der Atmosphare
~~Institute fur Physik der Atmosphare~~
8031 Weeling, Muencher St. 20
Oberpfaffenhofen D-8031 Webling/Obb.
West Germany A031

2) Sponsor Admin/Contractual Matters:

Dr. Poeplau
Deutsche Forschungs-und Versuchsanstalt
fur Physik der Atmosphare
Purchasing Dept., Central Purchasing Section
Postfach 90 60 58
5000 Koln 90
West Germany

Defense Priority Rating: N/A

Military Security Classification: _____

(or) Company/Industrial Proprietary: None

RESTRICTIONS

See Attached ----- Supplemental Information Sheet for Additional Requirements.

Travel: Foreign travel must have prior approval – Contact OCA in each case. Domestic travel requires sponsor approval where total will exceed greater of $500 or 125% of approved proposal budget category.

Equipment: Title vests with None proposed or anticipated

COMMENTS:

* Advance payment of $10,000 has been received. Per Article 5 of the Agreement, this advance payment will be applied to the final invoice and any remaining balance will be refunded at the end of the project.

Travel budget is limited to $10,000.

OCT 1982 RECEIVED Research Reports Office

COPIES TO:

RAN

~~Research Administrative Network~~ Research Security Services Research Communications (2)
Research Property Management ~~Reports Coordinator (OCA)~~ Project File
Accounting GTRI Other GTRI
Procurement/EES Supply Services Library Other _____

GEORGIA INSTITUTE OF TECHNOLOGY OFFICE OF CONTRACT ADMINISTRATION

SPONSORED PROJECT TERMINATION/CLOSEOUT SHEET

Date 12/12/85

Project No. A-3383 ~~School~~ Lab RAIL/IMD

Includes Subproject No.(s)

Project Director(s) E. F. Greneker GTRC ~~XXX~~

Sponsor Deutsche Forschungs-Und Versuchsanstalt

Title Technical Consulting During Development of an Instrument Coherent Polarization Diversity Meteorological Radar

Effective Completion Date: 5/31/85 (Performance) 5/31/85 (Reports)

Grant/Contract Closeout Actions Remaining:

- [ ] None
- [XX] Final Invoice or Final Fiscal Report
- [ ] Closing Documents
- [ ] Final Report of Inventions
- [ ] Govt. Property Inventory & Related Certificate
- [ ] Classified Material Certificate
- [ ] Other

Continues Project No. Continued by Project No.

COPIES TO:

Project Director
Research Administrative Network
Research Property Management
Accounting
Procurement/GTRI Supply Services
Research Security Services
Reports Coordinator (OCA)
Legal Services

Library
GTRC
Research Communications (2)
Project File
Other Jones

Heyser

FORM OCA 69.285

DFVLR POLARIMETRIC RADAR

TEST PROCEDURE OUTLINE:
AN INTERIM REPORT

Prepared for
Deutsche Forschungs-und Versuchsanstalt
fur Luft-und Raumfahrt e.v. (DFVLR)
8031 Wessling
Oberpfaffenhoffen, West Germany A031

Under Contract 55312-4337-82, Task II

by

E. F. Greneker, J. S. Ussailis, G. W. Ewell,
J. D. Echard, and R. C. Johnson

Georgia Institute of Technology
A Unit of the University System of Georgia
Engineering Experiment Station
Atlanta, Georgia 30332

December 1982

TABLE OF CONTENTS

TABLE OF CONTENTS (CONTINUED)

TABLE OF CONTENTS (CONTINUED)

LIST OF FIGURES

LIST OF TABLES

SECTION 1
INTRODUCTION

This report contains recommendations for testing the DFVLR polarimetric radar being developed by Enterprise Electronics Corporation (EEC), Enterprise, Alabama, USA. These test recommendations are based on a review of the technical proposal submitted by EEC to DFVLR and are intended to supplement the test plan outlined therein.

The test recommendations are presented in two general forms: (1) explicit test procedures and (2) suggested general test techniques that should be considered. Exact performance specifications are not included because: (1) we did not have the detailed EEC/DFVLR design documentation on hand to develop specific performance criteria, (2) funding and preparation time were limited, and (3) major changes to the DFVLR radar design can not be made at this time without a significant impact on system cost. Georgia Tech assumed that DFVLR had conducted a detailed system design and the specifications shown in the EEC proposal are adequate to meet DFVLR's research needs.

Specific tests and test methodologies for testing certain aspects of the DFVLR polarization diversity radar are presented in Sections 2 through 6. Each test recommendation was made with the full understanding that many design aspects of the DFVLR are fixed and can not be changed without a corresponding impact on the DFVLR developmental budget. Therefore, the exact tests to be specified must be determined by DFVLR.

SECTION 2
ANTENNA TESTS

2.1 OVERVIEW

The antenna tests should ensure that the antenna gain, sidelobe levels, and the overall polarization isolation specifications are met. The first set of antenna tests should encompass those normally performed on an antenna test range. A second set of tests should be specifically devoted to measuring antenna isolation and determining the entire cross-polarization sidelobe structure. The EEC planned rotation-about-axis measurement technique or a raster scanning technique can map the sidelobe structure.

The antenna should ideally be tested on an antenna measurement range which satisfies the $2\ d^2/\lambda$ criterion for separation between the test antenna and the source antenna. For an antenna diameter of 4.6 m (15 feet) operating at a frequency of 5500 MHz, the antenna separation should be 767 m (2515 feet). The Radiation Systems, Inc., antenna range in Sterling, Virginia is believed to have a path length of only 563 m (1800 feet). If this is correct, then an appropriate technique for measuring the antenna characteristics on this shorter range should be developed and verified. Re-focusing for the lesser range may be a solution and should be considered by Radiation Systems. They should verify that the selected techniques do provide accurate measurement of the co- and cross-polarized antenna patterns.

2.2 LIMITS OF CROSS-POLARIZATION MEASUREMENT

The peak of the cross-polarized beam should coincide with the first nulls in the co-polarized beam. Studies conducted at Georgia Tech have shown that (1) significant cross polarization extends beyond the region of the second sidelobes of the co-polarized beam and (2) measuring cross polarization from the co-polarized beam peak to the second nulls in the co-polarized beam will account for almost all antenna cross polarization. In the case of the DFVLR radar, antenna measurements should be conducted over the solid angle extending from the boresight axis to six degrees off boresight.

2.3 ANTENNA PATTERNS

The co-polarized and cross-polarized patterns should be simultaneously recorded. The power at horizontal and vertical output ports of the antenna should be recorded as the antenna is scanned from minus 6 degrees to plus 6 degrees across the boresight axis. A set of patterns must be recorded at each 10 degree plane of antenna roll around the boresight axis at frequencies of 5450, 5500, and 5550 MHz. The co-polarized boresight gain and the cross-polarized maximum gain should be measured and recorded at each of these frequencies.

A second technique may also be employed using a "raster scan" technique. An azimuthal pattern 12° wide (± 6° each side of boresight axis) and centered upon boresight may be taken each time the elevation axis is incremented one degree. The choice of either measurement technique is determined by the availability of antenna positioning equipment. The results of the two measurement methods should be similar.

2.4 VSWR

Swept frequency techniques should be employed to measure the VSWR of the antenna over the operating frequency band. VSWR is a significant measurement. Any reflected power from the antenna will be returned to the switch/polarizer and retransmitted in the orthogonal polarization channel. The resultant cross-polarized backscatter measurement is corrupted by this leakage of cross channel energy. From a knowledge of VSWR, the degree of data corruption can be reduced, in theory, by the application of an appropriate cancellation algorithm during data processing. If an algorithm to reduce corruption is not applied, the system performance limits are ascertained from the VSWR measurement.

2.5 MEASUREMENT OF ANTENNA POLARIZATION ISOLATION

One requirement of the DFVLR polarization diversity radar is it's ability to operate as a Circular Depolarization Ratio (CDR) meteorological measurement system employing the circular polarization mode of the antenna. All circular co-polarization and cross-polarization antenna information is calculable from linear polarization, if the antenna phase patterns are available. However, direct recording of the circular patterns is usually a preferable and quicker

method of antenna analysis. The direct recording of circular patterns is straightforward. The antenna should be configured for circular polarization, and the co-polarized and cross-polarized patterns should be recorded in the same manner as for linear polarization.

2.5.1 CIRCULAR POLARIZATION

The recommended technique for measurement of circular polarization requires many observations of precipitation while backscatter measurements are made. The resultant depolarization is graphed against the anticipated depolarization imposed by the shape of particles.[1] This curve asymptotically approachs the system integrated cancellation ratio if there is sufficient intra-channel receiver isolation. This value then becomes isolation for circular polarization after algebraic subtraction of 6 dB.

Two other possible schemes exist for the measurement of circular polarization isolation. One employs a measurement of the overall axial ratio of the antenna. This technique is very difficult to perform as it requires the elimination of almost all multipath on the antenna range; in the case of 30 dB isolation, the multipath energy must be reduced to - 53 dB with respect to the direct energy.[2]

The other possible technique exists in which the co-polarized and cross-polarized antenna patterns discussed in Section 2.2 are integrated and compared either manually or on a point-by-point basis using the antenna range computer. This technique is a straightforward measurement, but requires the same level of range cross-polarization sophistication as other techniques. However, it is the author's opinion that the required accuracy of cross-polarization isolation measurements are unattainable for circular polarization on the standard antenna range.

[1]Newell, R. E., Geotis, S. G., and Fleisher, A., "The Shape of Rain and Snow at Micro Wave Lengths", Research Report No. 28, Massachusetts Institute of Technology, Department of Meteorology, September, 1957.

[2]Ryan, C. E. "Review and evaluation of antenna test ranges" Letter report for Georgia Tech Project A-1729, Radar Division Engineering Experiment Station, Georgia Institute of Technology, 8 May 1975.

2.5.2 LINEAR POLARIZATION

Linear polarization isolation measurements are easier to perform on the antenna range since linear cross-polarization is not normally generated upon simple reflection. This is diametrically opposite to the case of circular polarization in which cross-polarization is generated at every reflection. For linear polarization, the integration method of calculating antenna isolation is recommended, however, care must be exercised to ensure that the range cross-polarization is considered and is reduced as much as practical.

SECTION 3
POLARIZATION SWITCH AND POLARIZER

3.1 VSWR

The polarization switch and polarizer VSWR should be measured using swept frequency techniques, rather than at three spot frequencies, because VSWR affects performance over the actual bandwidth of the received or transmitted signal and the three spot frequencies may only approximate the exact frequencies of operation. The DFVLR polarization switch is specified to have 30 dB isolation between channels; this requires an overall VSWR less than or equal to 1.065:1 at all four ports. Therefore, swept frequency techniques should be used to measure VSWR over the frequency range of 5440 MHz to 5560 MHz; the VSWR of each port should be less than or equal to 1.065:1 when all other ports are terminated with a load whose VSWR is less than or equal to 1.03:1.

3.2 ISOLATION, INSERTION LOSS, AND PHASE SHIFT

For both the linear and circular polarization modes, swept frequency techniques should be used to measure polarization switch isolation and insertion loss across the frequency range of 5440 MHz to 5560 MHz. These measurements should be made after the polarization switch temperature has stabilized. The polarization switch phase shift should also be measured using swept frequency techniques if the necessary instrumentation (network analyzer) is available. If the instrumentation is not available, a point-by-point measurement of forward and reverse phase shifts is acceptable, provided the frequency steps used are not greater than 0.5 MHz and anomalies do not occur.

3.3 TEMPERATURE RANGE

The polarization switch should be tested with the remainder of the microwave package before the units are installed in the radar to determine the effect of temperature on phase and amplitude tracking. Phase and amplitude should be monitored as the temperature is varied over the entire anticipated thermal operating range of these units. The temperature extremes under consideration should include the expected extremes of the environmental enclosure and the local heating effects of the enclosed microwave

components. An optimum tightly bounded temperature range that enables accurate phase and amplitude tracking should be found; this temperature range will in turn determine the thermal characteristics of the environmental enclosure.

An additional test should be performed after the polarization switch and microwave package are installed in the radar. The phase and amplitude tracking characteristics of the polarization switch and microwave package should be monitored from the time of initial transmitter turn on until the phase and amplitude tracking characteristics are stabilized. This stabilization time will determine the necessity for a minimum turn-on delay.

3.4 PHASE STABILITY AND REPEATABILITY

The polarization switch should be sufficiently tested to determine which components of phase stability and phase repeatability can be eliminated by signal processing (i.e., known components) and which components are properly in the domain of phase uncertainty (i.e., unknown components). The phase stability and phase repeatability must be measured separately. Phase stability measurements should be conducted over a reasonable time period to account for variations of temperature, pulse-to-pulse transmit power, and other factors that might cause instabilities. Repeatability measurements should be based solely upon the resetability of the polarization switch as it is switched between all phase steps to determine the components of the actual phase shift and the phase uncertainty contained therein. A graph of actual phase shift should be constructed from this information, and the correction data should be entered into the processor so that the values of phase shift can be corrected prior to processing actual meteorological data.

3.5 OTHER MEASUREMENTS

All specifications not specifically addressed here, but indicated in the EEC proposal of 30 September 1982, should be measured as indicated. Additionally, a reasonable test should be devised to ensure that the polarization switch assembly will not be damaged by a severe mismatch between this assembly and the antenna due to arcing in the waveguide or other catastrophic occurrence. The temporal length of this survivability need not significantly exceed the shut-down time of the transmitter.

SECTION 4
RECEIVER TESTS

4.1 OVERVIEW

Although the EEC proposal contains no receiver tests, the receiver must be tested because it is the heart of a polarization diversity measurement system. Two categories of receiver tests are necessary: (1) tests pertaining solely to polarization diversity operation and (2) tests pertaining to receivers in general. The polarization diversity tests should include intra-channel phase tracking, intra-channel amplitude tracking, non-linearity of the amplitude transfer function, and intra-channel isolation; minimum acceptable parameter values for circular depolarization ratio (CDR), linear depolarization ratio (LDR), differential reflectivity (Z_{DR}), and polarization null radars are listed in Table 1. The general tests should include dynamic range (DR), spurious free dynamic range (SFDR), noise figure (NF) or tangential sensitivity (TS), intermediate frequency bandwidth, and spurious responses.

TABLE 1. MINIMUM REQUIRED POLARIZATION DIVERSITY PARAMETERS FOR VARIOUS CLASSES OF METEOROLOGICAL RADARS

Parameter	Radar Class			
	CDR	LDR	Z_{DR}	Null
Receiver Intra-Channel Isolation	>50 dB	>45 dB	N/A	>45 dB
Intra-Channel Amplitude Uncertainty	1 dB	1 dB	N/A	UNK
Intra-Channel Phase Uncertainty	1 deg	1 deg	N/A	UNK
Non Linearity of Receiver Transfer Function	1 dB	1 dB	0.1 to 0.3 dB	UNK

UNK = Unknown

N/A = Not Applicable

4.2 POLARIZATION DIVERSITY RECEIVER TESTS

4.2.1 RECEIVER INTRA-CHANNEL ISOLATION

A test must be performed to measure isolation between the receiver channels. A pulse signal of approximately 1.0 μs length at the radar frequency of operation should be injected into one of the receiver channels. The pulse signal level should be set at approximately, but less than, the overall receiver 1 dB compression point. The output levels of the two logarithmic receiver channels should be measured; the outputs must differ by more than 50 dB for proper intra-channel isolation. The test should be repeated with the pulse signal injected into the other receiver channels.

4.2.2 INTRA-CHANNEL AMPLITUDE UNCERTAINTY

Intra-channel amplitude uncertainty tests should be conducted using the test configuration shown in Figure 1. The precision attenuator should be incremented in 1 dB steps as the outputs of both receiver channels are simultaneously recorded. Although linearity of the receiver channels should not be expected to correspond to linearity of the precision attenuator, the output levels of the two receiver channels must track within 1 dB.

4.2.3 PHASE UNCERTAINTY

The relative phase between two receiver channel output signals should be measured using the test configuration shown in Figure 2. As the RF phase shifter is adjusted over a 180 degree range, the phase of the signal at the output of each receiver channel must track within one degree. An alternative to this measurement employs the sampling of the receiver's in-phase (I) and quadrature (Q) outputs. For a 180 degree RF phase change, the I and Q outputs must deviate by no more than one degree from quadrature.

4.2.4 NON-LINEARITY OF THE AMPLITUDE TRANSFER FUNCTION

The non-linearity of the amplitude transfer function for the receiver channel that is to be utilized in the Z_{DR} measurements should be tested using the test configuration shown in Figure 3. When the precision attenuator is incremented in 0.1 dB steps over any 5 dB range within the receiver dynamic range, the output must not deviate more than 0.1 dB from linearity.

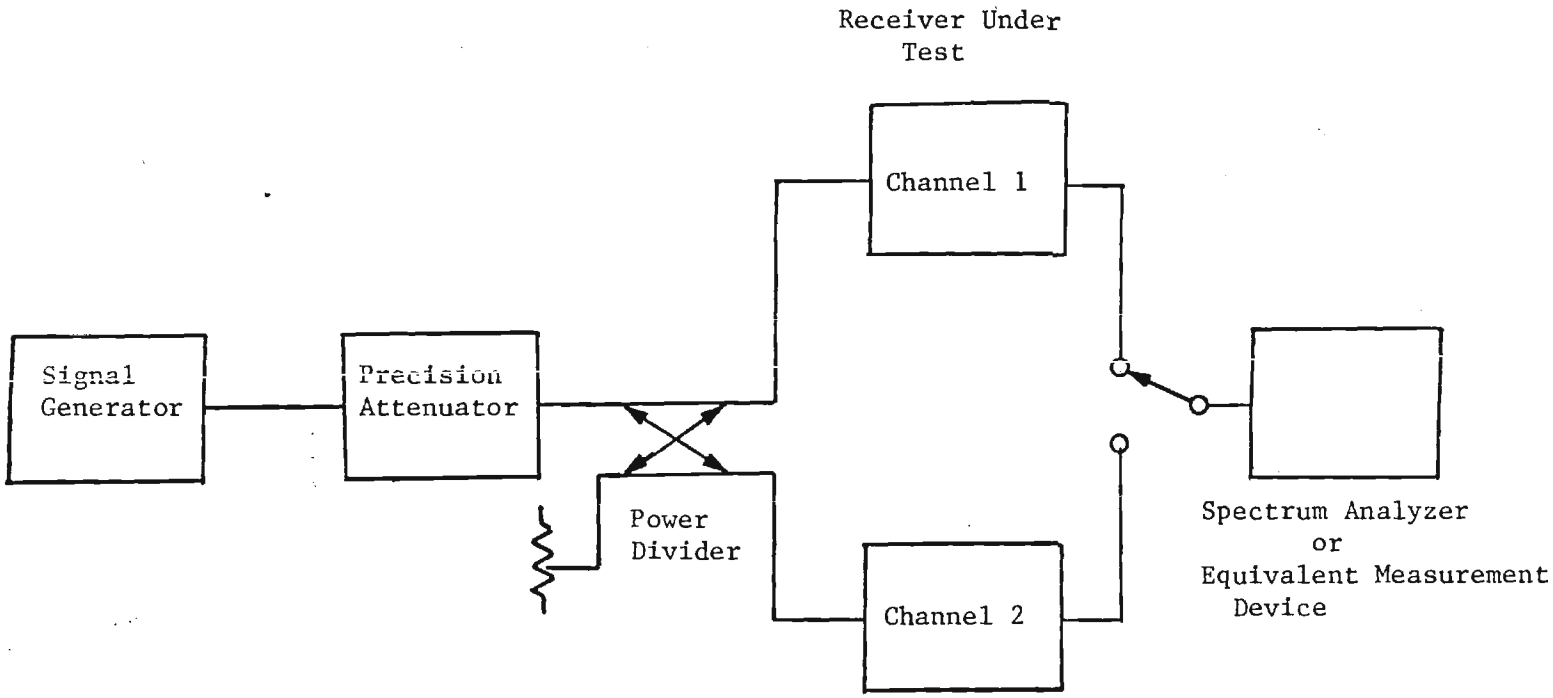

Figure 1. Test configuration for intra-channel amplitude tracking measurement.

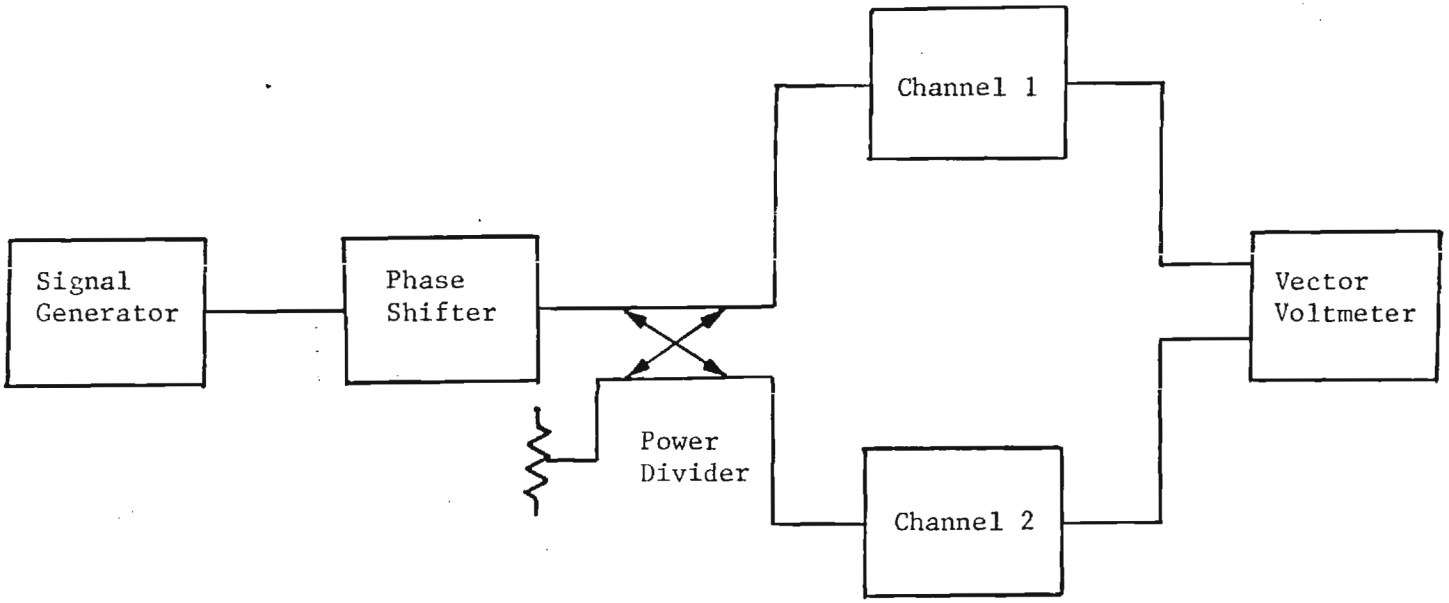

Figure 2. Test configuration for intra-channel phase tracking measurement.

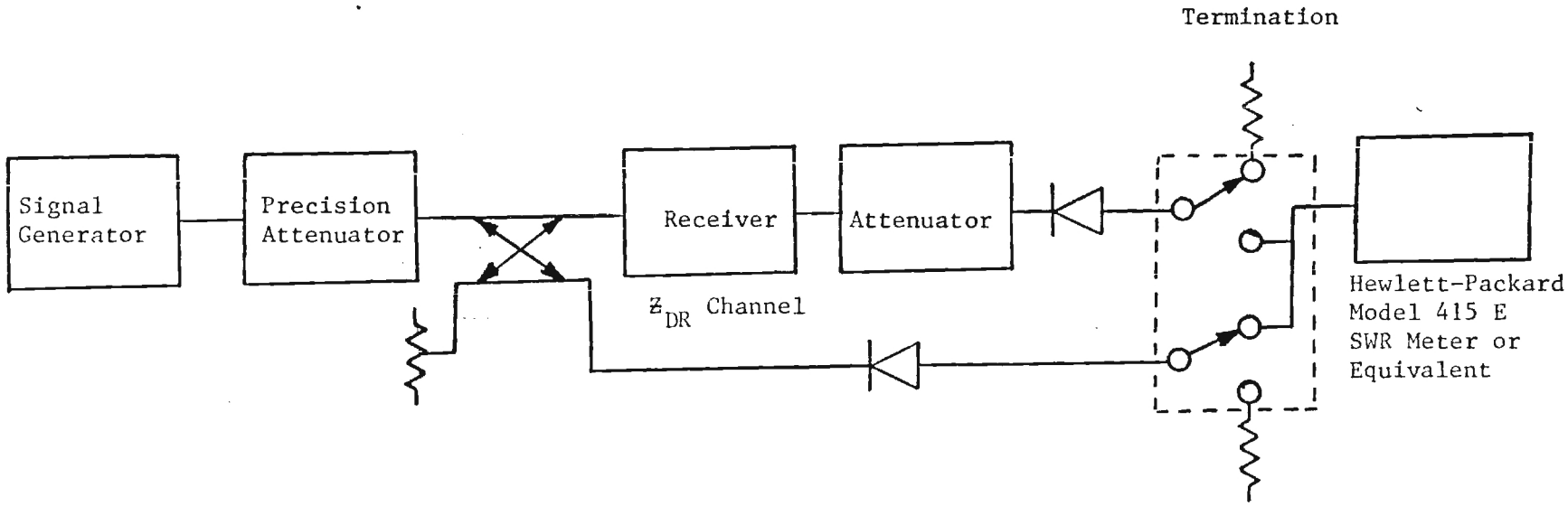

Figure 3. Test configuration for receiver transfer function.

4.3 GENERAL RECEIVER MEASUREMENTS

4.3.1 RF AND IF BANDWIDTH

Receiver RF and IF bandwidth tests should be conducted to determine the nature of the receiver passband, the output voltage levels, the system saturation levels, and the variations in bandwidth with changes in input signal strength. RF bandwidth tests should be conducted at each of the center frequencies. IF bandwidth tests should be conducted for each selectable bandpass. These tests must encompass a range of input power levels from the 1 dB compression point to approximately 10 dB above the noise floor. The exact dynamic range and anticipated bandwidth should be a function of the transmitted pulse width.

Receiver RF bandwidth tests should be conducted using the test configuration shown in Figure 4. An oscilloscope display and camera can be used in lieu of the X-Y recorder to record results. The sweep generator should be set for an appropriate sweep width centered about the frequency of interest. The receiver should be tuned to the center frequency. The detected receiver output should be recorded as a function of input frequency as the input power is stepped downward in 10 dB increments from the 1 dB receiver compression point to approximately 10 dB above the noise threshold. The recorded data must be carefully annotated to correlate the output voltage levels with the input swept frequency range and input signal levels.

The receiver IF bandwidth tests should be conducted using a test configuration similar to that used for the RF bandwidth tests. Examples of anticipated 3 dB IF bandwidths as a function of transmitted pulse widths are presented in Table 2. The IF passband for each transmitted pulse width should be characterized to determine the -3 dB points, and the skirt selectivity for each passband should be analyzed for proper width and shape to ensure proper measurement of pulse signals as well as minimum phase dispersion.

4.3.2 RECEIVER DYNAMIC RANGE TESTS

The receiver should be tested to determine the dynamic range for both the linear and logarithmic outputs. The dynamic range should be determined by measuring the difference between the receiver noise floor level and the 1 dB compression point when the widest IF passband is selected. (The 1 dB

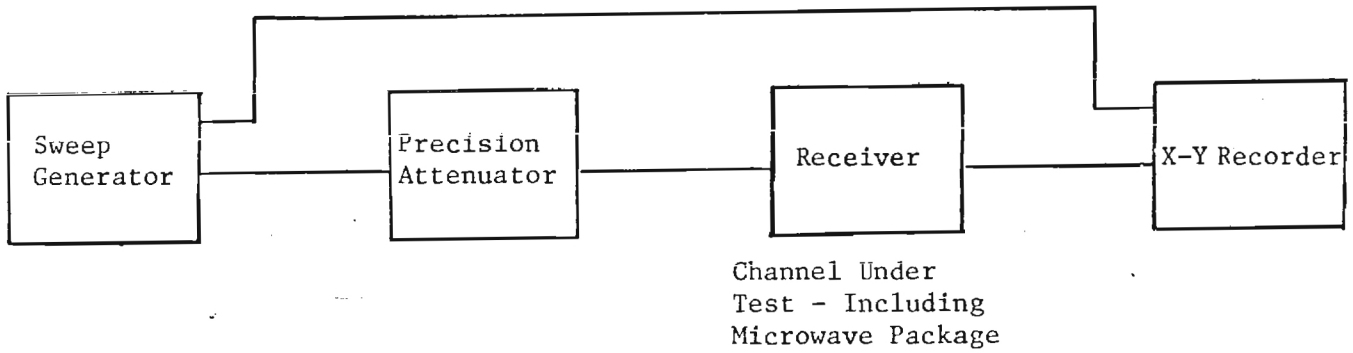

Figure 4. Test configuration for RF bandwidth characterization scheme.

compression point is defined as the point at which 1 dB of non-linearity is observed at the output for a linear increase in input signal level.) The effectiveness and calibration curve of the automatic gain control (AGC) or sensitivity time control (STC) circuit should be verified during the dynamic range test.

TABLE 2. RECEIVER -3 dB IF BANDWIDTH FOR VARIOUS TRANSMITTED PULSE WIDTHS

Transmitted Pulse Width (μs)	Receiver 3 dB Bandwidth (MHz)
2	1.2
1	2.4
0.5	4.8

4.3.3 RECEIVER INTERMODULATION DISTORTION TEST

The receiver should be tested to determine the level at which intermodulation products are processable, even if preselection is employed. A two-tone intermodulation distortion test should be conducted using the test configuration shown in Figure 5 to determine the intercept point. The intercept point can be used in conjunction with the minimum detectable signal level and the nomogram shown in Figure 6 to determine detectable intermodulation product signal levels.

4.3.4 RECEIVER LOCAL OSCILLATOR SPURIOUS RESPONSE TEST

The receiver should be tested to determine whether the local oscillator introduces spurious responses. This test can be conducted using a test configuration similar to that used for the RF bandwidth test (Figure 4), but the sweep width should be increased to cover the local oscillator circuit frequency. The receiver output as a function of input frequency for various input signal levels should be recorded.

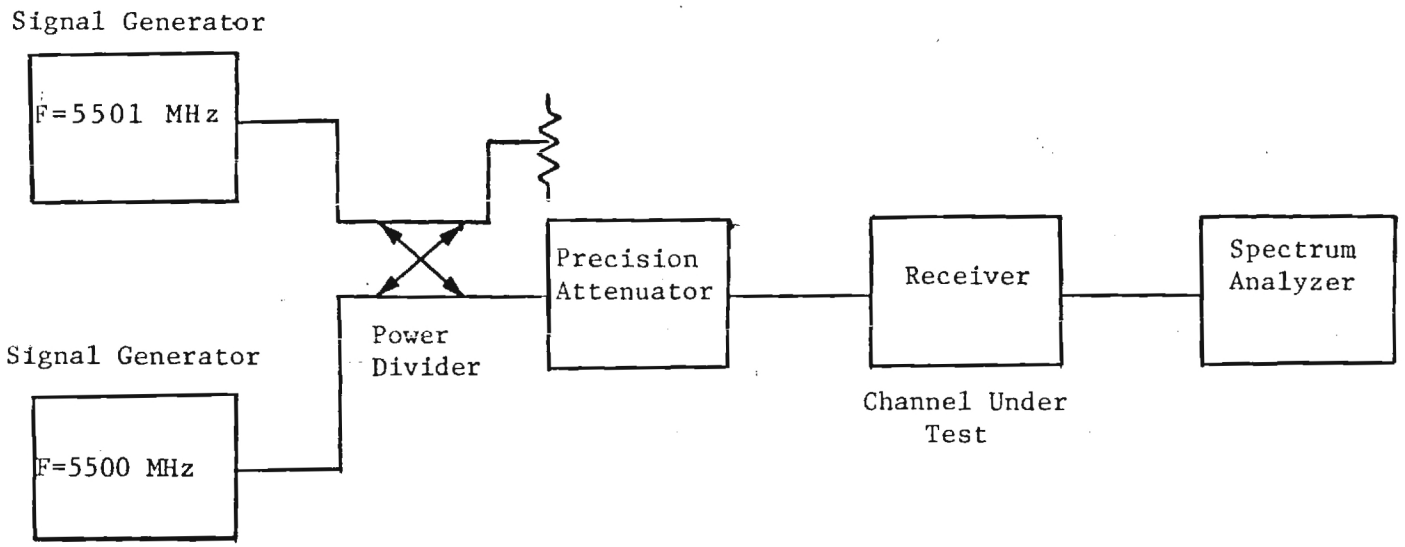

Figure 5. Test configuration for intercept point measurement.

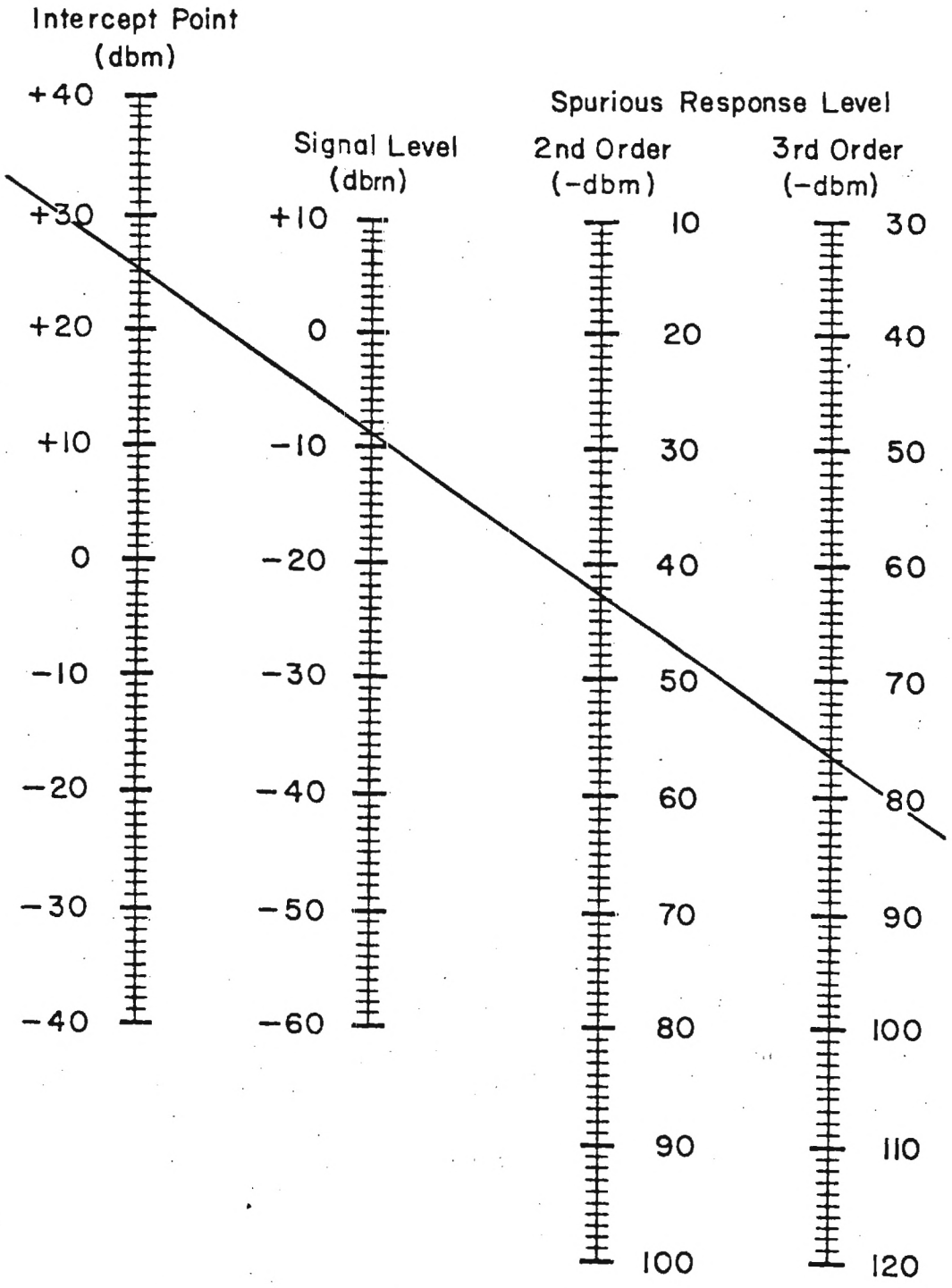

Figure 6. Intermodulation distortion nomograph from Electronic Design, 1 February 1967. The diagonal line indicates the intercept point for a typical low-noise amplifier (LNA) and the resultant level of processable intermodulation products.

4.3.5 RECEIVER SENSITIVITY OR NOISE FLOOR TEST

Various equivalent measurements of system sensitivity can be used to determine the receiver noise floor or minimum discernible signal (MDS). The receiver tangential sensitivity should be measured using the test configuration shown in Figure 7. Although this measurement is reasonably repeatable, at least two different persons should perform the measurement at each frequency to establish an average value for tangential sensitivity; this average value should be used as the measured tangential sensitivity. The receiver noise floor or minimum discernible signal can then be determined from the following relationship:

$$Nf = 114 \text{ dBm} - (TS + 10 \log (2BV)^{1/2} + C) . \qquad (10)$$

Where: Nf = noise figure in dB
TS = tangential sensitivity in dBm
B = IF bandwidth in MHz
V = video bandwidth in MHz
C = tangential sensitivity conversion constant of 6 dB*

4.3.6 RECEIVER FREQUENCY STABILITY AND RESETABILITY

Receiver frequency stability and resetability should be tested. The measurement is straightforward since the IF frequency is fixed. The local oscillator frequency should be compared with that of a frequency standard. Both long term and short term stability of the local oscillator should be examined to determine the receiver characteristics and to establish an effective recalibration cycle.

Frequency resetability is less a function of the reference standard than a function of the phase locked loop and oscillator driver circuitry. For the frequency resetability tests, the receiver should be initially tuned to a midband reference frequency, then displaced to the band edge, and finally returned to the reference frequency. The amount of frequency reset error should be recorded for both manual and automatic tuning.

*Various values between 6 and 8 dB for this constant may be found in the literature. This discrepancy may present small noise figure error.

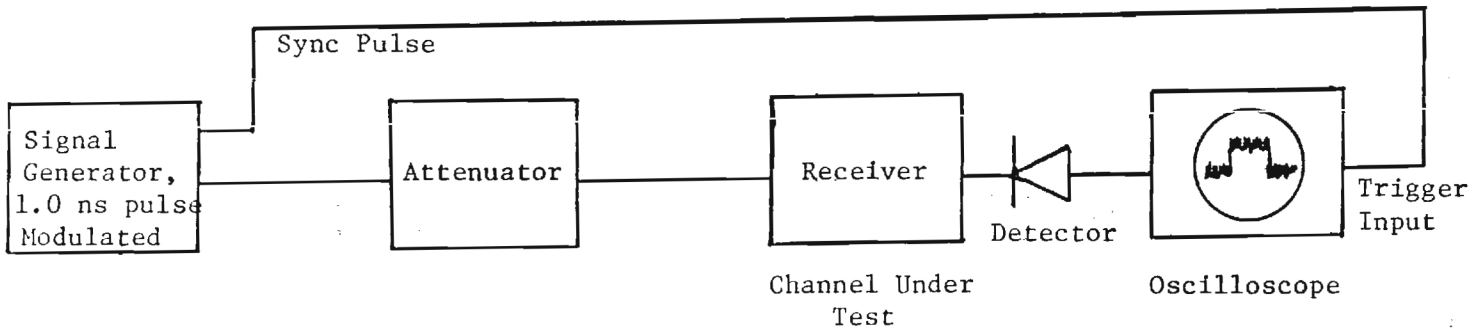

Figure 7. Test configuration for tangential sensory measurement.

SECTION 5
TRANSMITTER TESTS

5.1 OVERLOAD AND PROTECTIVE CIRCUITS

The transmitter should be tested to demonstrate that it contains the overload and protective circuitry necessary to adequately protect the magnetron and ensure reliable magnetron operation. Although many of these tests are not part of either the proposal or the specification, their inclusion is necessary to ensure reliable system operation.

5.1.1 WAVEGUIDE PRESSURE

This test should demonstrate that lack of adequate waveguide pressurization prevents the system from radiating power. The demonstration should show that: (1) loss of waveguide pressure when the transmitter is on causes the transmitter to revert to standby status and (2) inadequate waveguide pressure prevents the system from being placed in a radiate condition.

5.1.2 VSWR

This test should demonstrate that excessive VSWR (or equivalently excessive reflected power from the antenna) will cause the system to revert to a standby condition. These tests should be conducted by simulating the excessive VSWR condition, rather than actual insertion of a high VSWR for test purposes.

5.1.3 SHORT CIRCUIT TESTS

Since magnetron or modulator malfunctions may result in an extremely low impedance at the modulator output, operation into a short circuit should be demonstrated. The magnetron should be removed from the modulator and the system should be operated into a resistive load for this test. The load should be shorted to ground; satisfactory operation should be indicated by a lack of damage to any modulator components and a prompt reversal of the transmitter to the standby condition.

5.1.4 OPEN CIRCUIT TESTS

Since magnetron malfunctions may result in an abrupt increase in magnetron impedance, operation in such a mode must be avoided to prevent magnetron damage. Protection against such conditions is necessary for reliable operation. The magnetron should be removed for the open circuit test. The modulator should be operated into an open circuit while the output voltage is monitored with a high voltage oscilloscope. Proper operation should be indicated by (1) firing of the over-voltage spark gap to prevent excessive voltage across the magnetron and (2) prompt reversal of the transmitter to the standby condition.

5.1.5 EXCESSIVE MAGNETRON CURRENT OVERLOAD

Operation of the magnetron current overload circuit should be demonstrated. Due to the wide variety of possible circuit configurations, it is difficult to provide exact guidance of the details of the test; however, any test performed should demonstrate that operation of the magnetron beyond its normal performance limits is excluded.

5.1.6 EXCESSIVE SHUNT DIODE CURRENT

Since shunt diode current is a relatively sensitive function of the load characteristics, protection from this overload should also be demonstrated. The same cautions expressed in Section 5.1.5 above should be observed for this test.

5.1.7 PROPER HEATER SCHEDULE

The correct reduction in heater voltage as a function of duty cycle and transition from the standby condition to the radiate condition should be demonstrated.

5.1.8 POWER SUPPLY OVERLOAD

The operation of an overload circuit which prevents excessive amounts of current from being drawn from the power supply should be demonstrated to ensure protection of the modulator components.

5.2 MAGNETRON FUNCTIONAL TESTS

Described in this section are a series of tests designed to demonstrate the proper values and ranges for major magnetron functional parameters. In addition, these tests provide a reference for the calibration subsystem included as part of the overall radar system.

5.2.1 FREQUENCY

These tests should demonstrate that the magnetron meets all of its functional requirements over the frequency range of 5450 to 5550 MHz. Although actual measurements at the band edges and band center are considered adequate, the tube should also be tuned throughout its operational frequency range while the output is carefully monitored for signs of excessive power variation or presence of moding at specific frequencies.

5.2.2 PEAK POWER OUTPUT

The transmitter power output and power output from the two arms of the polarization network should be measured. The total power output should be greater than 300 kW. The preferred test method is to measure the power output by using a microwave peak power meter. The power output can also be determined by measuring average power output and duty cycle, and then computing peak power based upon measured pulse characteristics.

5.2.3 PULSE WIDTH AND STABILITY

The transmitter pulse width for each of the three modes should be measured by using an oscilloscope to observe the detected RF output from the transmitter. In addition, short term variations in pulse width should be recorded, and their conformance with the stability error budget discussed in Section 5.3 should be demonstrated.

5.2.4 PULSE REPETITION FREQUENCY

The transmitter PRF for each of the three modes should be measured by using an oscilloscope to observe the detected RF output from the transmitter. The PRF in each of the three modes should be within 10% of the nominal value.

5.2.5 TIME DELAY STABILITY

The detected RF pulse and the system timing pulse should be displayed simultaneously on an oscilloscope. The variations in time delay between these two signals should be compatible with the stability budget discussed in Section 5.3.

5.2.6 AMPLITUDE STABILITY

The detected RF output pulse from the transmitter should be observed on an oscilloscope. Variations in amplitude of the displayed pulse should be compatible with the stability budget discussed in Section 5.3.

5.3 OVERALL TRANSMITTER PHASE TESTS

These tests are designed to ensure that the system has the intrinsic capability required for measurement of the desired phase variations over the entire operating envelope. The initial requirement is to establish a stability budget by outlining all of the factors which contribute to the accuracy limitation of phase measurements in the system and assigning reasonable values to each factor. The contributions of each of these factors to the overall phase stability should be measured to demonstrate that the individual components are well controlled. Then, the actual phase stability of the overall system should be measured. These measurements should identify those truly random errors on a pulse-to-pulse basis as well as those errors which are either increasing or decreasing functions of range to the target.

5.3.1 STABILITY BUDGET

The manufacturer should establish an error budget of the primary factors which contribute to phase noise and phase measurement inaccuracies. These factors should include amplitude stability, pulse width stability, time delay stability, stable local oscillator (STALO) frequency stability, coherent oscillator (COHO) frequency stability, and random COHO phase lock errors.

5.3.2 STALO FREQUENCY STABILITY

The STALO frequency stability should be determined by measuring the sidebands induced by phase noise. The frequency stability should be compatible with the error budget.

5.3.3 MAGNETRON FREQUENCY STABILITY

The stability of the magnetron should be determined by measuring the variations in the voltage output from the automatic frequency control (AFC) discriminator; the AFC voltage should be a measure of variations between the magnetron frequency and the STALO frequency.

5.3.4 OVERALL PHASE STABILITY

The overall phase stability can be determined by measurements that are internal to or external to the radar. These measurements must be conducted in such a manner that the random phase components and the range dependent components are separated and the overall phase measurement stability is indicative of that which would be obtained over the entire range of target ranges to be encountered. Since these measurements are sensitive to fluctuations in the phase as well as average values, both average and RMS values of the phase variations should be measured.

5.3.4.1 External Phase Stability Measurements

Overall system phase stability can be demonstrated by external phase stability measurements conducted by using a standard target if the following conditions are met: (1) the propagation medium must be essentially stationary and homogeneous so as not to affect the measurement capability, (2) measurements must be made at several ranges to identify both the range dependent and range independent components, (3) the signal-to-clutter and signal-to-noise ratios must be sufficiently large to achieve the desired phase accuracies (approximately 26 dB is required for 3^{o} phase measurement accuracy), and (4) the beamwidth and location of the reflector must be such that multipath returns are minimized.

5.3.4.2 Internal Coherence Measurements

Determination of phase measurement accuracy by measurements conducted internal (rather than external) to the radar has a number of advantages including ease of measurement, independence from external weather conditions, ability to operate without fixed external targets, and capability to make measurements regularly throughout the measurement program. The major disadvantage is the additional equipment required for such measurements.

Internal cohere or several values of
delay (to identify t or) and might involve
the use of acoustic uencies to delay the
transmitted pulse to This delayed pulse is
then reinjected in is measured. The
observations about he signal generation
process and in the 3.4.1, also apply to
internal measurement rage values of phase
differences should coherence tests, and
measurements at two lesirable.

SECTION 6
RADAR SIGNAL PROCESSOR TESTS

6.1 OVERVIEW

The following tests are recommended in addition to those tests outlined in Section 9.4 of technical proposal P-1038-81/82. The tests recommended in this section will demonstrate the proper functioning of not only the digital signal processor (DSP), but also the entire radar system. Thus, these tests establish measurement accuracies and resolutions of the DSP only if the rest of the radar system has been tested independently and found to meet the required specifications.

The DSP tests utilize three types of targets: static targets, dynamic targets, and targets of opportunity. The first two types of tests employ calibrated radar reflectors. For the static test, the reflectors are fixed in position. For the dynamic tests, the reflectors are moving. The static and dynamic tests are tailored to provide testing of some part or function of the signal processor. Tests utilizing weather targets of opportunity are also recommended. A summary of DSP features to be tested is provided in Table 3. The specified tests called for in this table are described below in detail.

6.2 STATIC TESTS

The static tests are conducted by using calibrated corner reflectors placed in the first range cell (range of 1 km). The reflectors should each have a radar cross section of about 250 m^2 (24 dBsm) to provide sufficient signal-to-clutter ratio (20 dB) in this cell. The clutter level at this range with a 1 degree beamwidth is estimated to be +4 dBsm; this estimate is based on assumptions that the normalized radar cross section for a grassy open field is -30 dBsm (worst case) and the grazing angle is low (radar on a tower).

The clutter rejection filter in the DSP must be inhibited during these tests since returns from the stationary corner reflectors should show up in the zero Doppler bin of the FFT output. When a trihedral reflector is placed in the range cell, measurement of reflectivity (Z) accuracy and system linear polarization isolation should be possible. With the clutter rejection filter active, the clutter rejection capability of the DSP can also be demonstrated.

TABLE 3
DATA SIGNAL PROCESSING TEST

Tests / DSP Features	Static Tests	Dynamic Tests	Weather Tests (Extended Target in Range & Azimuth)
Real-time operation of FFT (32, 64, 128 points)		X	X
Clutter Rejection	X	X	X
Velocity Estimate (V)		X	
Spectral Width Estimate (O)		X	
Reflectivity Estimate (Z), (Z-C)	X	X	
Scattering Matrix Estimates (Four Complex-Valued Quantities)	X	X	
System Polarization Performance	X	X	
System Cross-Polarization Performance	X	X	

A dihedral reflector can be placed alone in the range cell and canted at various angles to provide linear cross-polarized returns. For example, if the canting angle is $+45^{o}$ and vertical polarization is transmitted, the return polarization should be $+90^{o}$; that is, horizontal polarization should be returned. This should allow testing of the cross-polarization channel. Other polarization angles can be provided by canting the dihedral reflector at various geometric angles. In general, the polarization angle of the radar return relative to the transmit polarization is equal to twice the canting angle of the dihedral reflector if vertical or horizontal polarization is transmitted. Tests can thus be devised to obtain any single element of the scattering matrix while the remaining elements are theoretically zero valued.

6.3 DYNAMIC TESTS

The dynamic tests are conducted by using several corner reflectors on a rotating arm as illustrated in Figures 8 and 9. The arm is mounted on a pole or small tower and driven by a motor. The tangential velocity of the reflector at each end of the arm is related to the arm radius (ℓ) and rpm as

$$V_t(m/s) = \frac{\pi \ell(m)}{30} \cdot rpm \cdot$$

Thus, the maximum Doppler frequency shift at 5.5 GHz due to the rotation of the arm is given by

$$\text{Max } f_d \text{ (Hz)} = \frac{2V_t(m/s)}{3\text{x}10^8 \text{ m/s}} \text{ x } 5.5 \text{ x } 10^9 \text{ Hz}$$

or

$$\text{Max } f_d \text{ (Hz)} = \frac{110\pi}{90} \cdot \ell(m) \cdot rpm$$

If an arm radius of 5 meters is used, then the rpm needed to achieve the maximum unambiguous Doppler shift for each PRF is as listed in Table 4.

The testing of the signal processor at maximum unambiguous Doppler shift is not required for all PRF rates. Hence, a reasonable arm rotation rate is about 10 rpm (one revolution every six seconds).

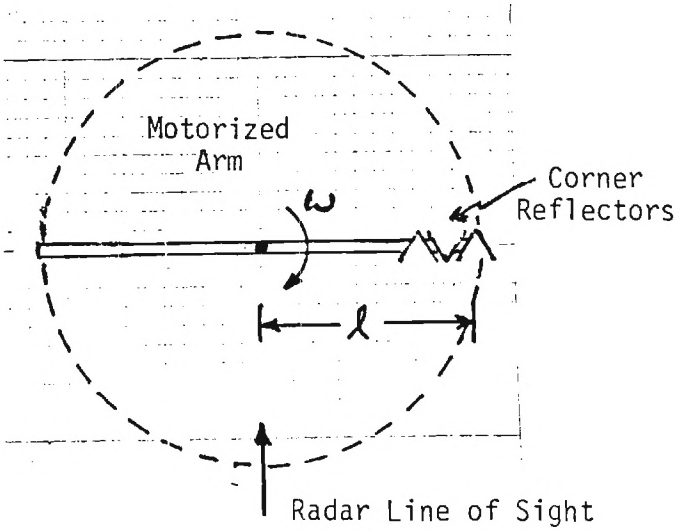

Figure 8. Top view of motorized arm and attached corner reflectors. At 10 rpm, one period of rotation is six seconds.

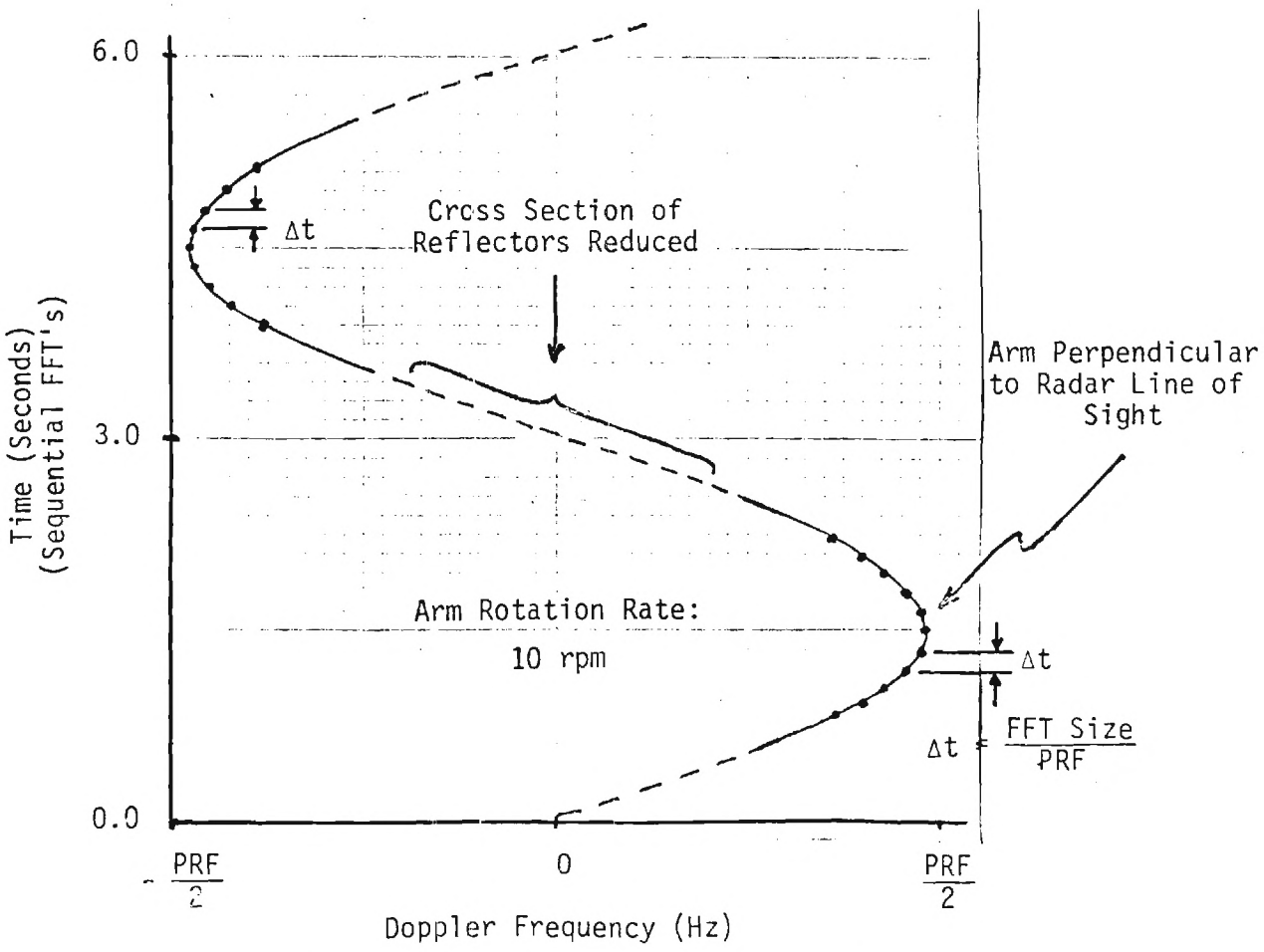

Figure 9. Variation of corner reflector Doppler frequency with time. Time separation between sequential FFT's defined as Δt.

TABLE 4. RELATIONSHIP BETWEEN TARGET SPEED AND DOPPLER FREQUENCY SHIFT

PRF (Hz)	RPM	V_t (m/s)
400	10.4	±5.45
1,200	31.2	±16.34
2,400	62.4	±32.67

Reflectors located at positions along the arm experience velocities that are slower than those listed in Table 4. For example, a reflector located at the center of the arm does not experience any tangential velocity component, even though it does rotate. By appropriately positioning combinations of reflectors (trihedrals and dihedrals), various spectral situations can be simulated. Reflectors of about 25 m^2 (14 dBsm) cross-section should be adequate for the dynamic tests since ground clutter is at essentially zero Doppler.

As the arm rotates about its pivot, the corner reflectors should travel around a circular path and experience a velocity relative to the radar that varies sinusoidally with time. Therefore, the Doppler frequency shift measured at the DSP output should also vary sinusoidally with time as illustrated in Figure 9. In this figure, only the velocity trajectory of a pair of corner reflectors mounted back-to-back is shown. As the reflectors turn relative to the radar, their radar cross-sections also vary. The maximum cross-section and maximum Doppler shift are exhibited when the arm is perpendicular to the radar line of sight. The reflector cross-section remains fairly constant (a 10 dB variation) over a ±30° sector about this point. At other angles, the cross-section of the corners and arms should be much lower. The arm and back of the reflectors should be covered with radar absorber material to minimize their cross-section contributions.

Since a specified number (32, 64, or 128) of radar returns from one range cell is required to provide a Doppler "picture" of that cell, the time between Doppler pictures, Δt, is given by

$$\Delta t = \text{FFT size/PRF}.$$

The separate Doppler pictures are indicated in Figure 9 as dots superimposed on the sinusoidally varying function. Of course, each dot only represents one part of the entire spectrum that is displayed.

Combinations of reflectors can be used to simulate spectral shapes which should test the DSP's spectral width estimation algorithm and the spectral resolution. A single reflector should allow verification of velocity estimation and reflectivity measurement accuracies.

The degree of clutter rejection achieved over a given bandwidth can be measured by mounting several corner reflectors close to the pivot point on the rotating arm. The velocity of the corner reflectors can, thus, be made arbitrarily small to appear as clutter moving in the wind. Additional reflectors can be mounted to appear as low velocity weather.

Real time operation of the FFT processor within a single range cell can be tested by observing the Doppler trajectory of a corner reflector mounted on the rotating arm. Since the arm rpm and radius are known, one can determine how often the FFT's are being performed.

6.4 WEATHER TESTS

Weather targets of opportunity provide the only feasible extended targets that can realistically be used to demonstrate the real-time operation of the DSP over a large range and azimuth area. However, this type of test is not useful for verifying the accuracy to which the DSP can estimate various spectral quantities. Therefore, static and dynamic tests utilizing calibrated reflectors are necessary.

The tests outlined in Section 9.4.2 of the technical proposal P-1038-81/82 in which weather is used as a test target should be suffieient. No additional tests are recommended.

the antenna. It was suggested that antenna surface deformation due to slewing could affect the polarization characteristics of the antenna. EEC took the position that this analysis was not part of the contract.

5. Welded Waveguide: Georgia Tech suggested that the waveguide running between the feed and along the feed arm support structure be welded at various intervals. Welding is proposed to reduce differential expansion between feed lines.

6. Infra-Red Heating of Feed: There was concern that infra-red energy from the sun would be focused on the feed if the antenna was accidentally pointed at the sun, and the resultant heating would deform the feed. EEC will investigate this problem.

7. Standing Wave Ratio (SWR) Versus Isolation: EEC plans to specify the SWR of the polarization network (switch) and associated microwave circuitry on the basis of measurements made on the component as individual parts. Georgia Tech suggested that the polarization specification be tested for the entire system after the system is assembled. EEC suggested that a double stub tuner be used as a nulling network to lower the specified SWR. The issue of testing SWR is unresolved.

8. Slip Rings Versus Coiled Coaxial Cable: EEC will use coiled coaxial cables to connect the antenna-mounted receiver components to the system at the antenna pedestal. EEC argued that the substitution of coaxial slip rings would cost $10,000 to install and that this was beyond the contract specification.

9. Flexguide Between Antenna Feed and Waveguide Run: EEC had planned to use a short section of flexible waveguide near the antenna feed to adjust the phase between channels. After discussion it was agreed that this design was not a good idea. EEC will investigate other ways of achieving the phase trim between channels.

10. Switching of Receiver Channels: There was a discussion concerning the desirability of switching receiver outputs on a pulse-to-pulse basis instead of switching the microwave network high powered switch when making certain measurements. It was finally determined that the microwave switch must be switched instead of the receiver output. This determination was made after EEC discussed switch specifications with the manufacturer.

11. Handwheels and Locking Pins on Antenna: Georgia Tech suggested that handwheels be supplied with the antenna to allow movement during power failures. EEC countered that the antenna could be stowed by one man using the leverage of the counterbalance. If this is not the case, there may be problems stowing the antenna should a power failure occur during use. EEC agreed that the provision of locking pins would be a good idea.

12. High VSWR Protection: The system design presented at the meeting did not provide for transmitter "shut down" if the switch or other components in the microwave network should encounter high VSWR conditions due to arcing or other problems. EEC agreed to move the reflected power monitor point to a location in the transmitter output that would allow a high VSWR in the microwave network to be detected and thus protect the polarization by shutting down the transmitter under high VSWR conditions.

13. Local Oscillator Run-Out Time: The local oscillator is phase locked to the transmitted pulse. The stability of the phase lock (with increasing time) after transmitter firing was questioned by Georgia Tech. Georgia Tech will obtain the stability specification on the local oscillator and provide it to DFVLR.

14. Overall Receiver Sensitivity: The specification on the receiver minimum detectable signal was questioned by Georgia Tech. The specified receiver bandwidth was half the required bandwidth. It was also pointed out that increased receiver bandwidth would be desirable to reduce the phase dispersion that will occur if the presently specified bandwidth is utilized. The minimum detectable signal level will drop 3 dB if the bandwidth is increased to improve phase dispersal. It is suggested that DFVLR conduct analysis on the trade-offs involved regarding receiver bandwidth versus measurement precision.

15. Receiver Gain Settings: The present EEC signal processor will not control the gain of each receiver separately. This may be a problem when the power returned to one channel is 30 dB below the power in the other channel. For certain measurements, it may be useful to increase the gain in the "low" channel by a known amount. This differential treatment would be possible if EEC can make a software modification and add an additional output port to drive the additional Sensitivity Time Control circuit (STC).

16. Use of Transponder With Radar: The use of a standard transponder or radar beacon will not be possible because of the instability problem that would occur if the local oscillator signal were moved in "side step" fashion. Thus the DFVLR aircraft conducting cloud physics sampling missions must be located using means other than a radar beacon.

17. Scattering Matrix: Dr. J. D. Echard has developed a review of the scattering matrix that will be provided by the EEC signal processor. This discussion is included as Attachment I to this letter.

These are the major points that were part of the EEC/DFVLR meeting summary. A written meeting summary was prepared by EEC and agreed on by the DFVLR representative on the last day of the review. This report addresses many points of the official meeting summary.

It is our understanding that the next effort that Georgia Tech is to undertake within the next 60 days is the review of the EEC final specifications document. This review is to be completed in preparation for the 18 July system design review to be held at Georgia Tech. If there are questions pertaining to this report, please feel free to call me at (404) 424-9616 between 1300 and 2100 DMT.

Yours truly.

Gene Greneker
Project Director

cc: EKR, JLE, NTA, HLB, JDE, JSU, OCA

Attachment I

Discussion on the Derivation of the Scattering Matrix to be Used by the DFVLR Signal Processor

5/24/85
JDE

Problem: Estimation of Scattering Matrix Elements With a Coherent-on-Receive Radar

Approach:

Figure 1 indicates the transmit-receive timing of the radar. As indicated, orthogonal polarizations are transmitted on alternate pulses at the pulse repetition rate (PRF). Both orthogonal polarized signals are received simultaneously via channels a and b. The nature of the received pulses is shown in Figure 1 for only one range cell - the ith range cell. Since the modulation on each returned pulse can be considered complex valued (A and ϕ or I and Q), with two pulse tranmissions all the information on the scattering marix is obtained -- A_{aa}, ϕ_{aa}, A_{ab}, ϕ_{ab}, A_{ba}, ϕ_{ba}, A_{bb}, and ϕ_{bb}. However, the returns from a pair of transmitted pulses are not sufficient for determining the velocity of the target (Doppler). A number of transmitted pulse-pairs is needed to estimate the target Doppler.

The diagrams shown in Figures 2 and 3 indicate how the scattering matrix elements can be extracted as a function of Doppler shift. Figure 2 indicates typical receive channels with explanations of the frequency and phase terms involved. Note that the video signals (out of the A/D converterss) are independent of transmitter frequency and phase. However, the video signal is still dependent on target position (velocity) and the target reflected phase (the information desired).

Figure 3 indicates how the I and Q signals from both receive channels can be used to extract polarimetric phase as a function of Doppler frequency. Note that the same Doppler phase exists on each of the two receive signals. However, the Doppler phase will be differrent for the next pair of receive signals obtained when the next pulse is transmitted.

The output quantities shown in Figure 3 can be placed in matrix form as follows:

$$S_j = \begin{bmatrix} A_{jaa}e^{j\phi_{jaa}} & A_{jab}e^{j\phi_{jab}} \\ A_{jba}e^{j\phi_{jba}} & A_{jbb}e^{j\phi_{jbb}} \end{bmatrix}$$

1st transmission <——

2nd transmission <——

Where subscript "j" refers to Doppler spectrum component #j (j = 1,2 ...m). The first row of the above scattering matrix is obtained from the circuit of Figure 3 when polarization "a" is transmitted. The second row is obtained when polarization "b" is transmitted in the next pulse repetition period (see Figure 1).

Since absolute phase is not important, one of the phases can be removed from the scattering matrix as indicated below:

$$S_j = e^{j\phi_{jaa}} \begin{bmatrix} A_{jaa} & A_{jab} e^{j(\phi_{jab} - \phi_{jaa})} \\ A_{jba} e^{j(\phi_{jba} - \phi_{jaa})} & A_{jbb} e^{j(\phi_{jbb} - \phi_{jaa})} \end{bmatrix}$$

This operation is not shown in Figure 3, but is easily performed from the information available. Note that there is no Doppler phase in the $(\phi_{jab} - \phi_{jaa})$ term, but there is a Doppler phase in the $(\phi_{jba} - \phi_{jaa})$ and $(\phi_{jbb} - \phi_{jaa})$ terms which must be estimated and removed.

FIGURE 1.
TRANSMIT – RECEIVE TIMING

a, b = orthogonal polarizations

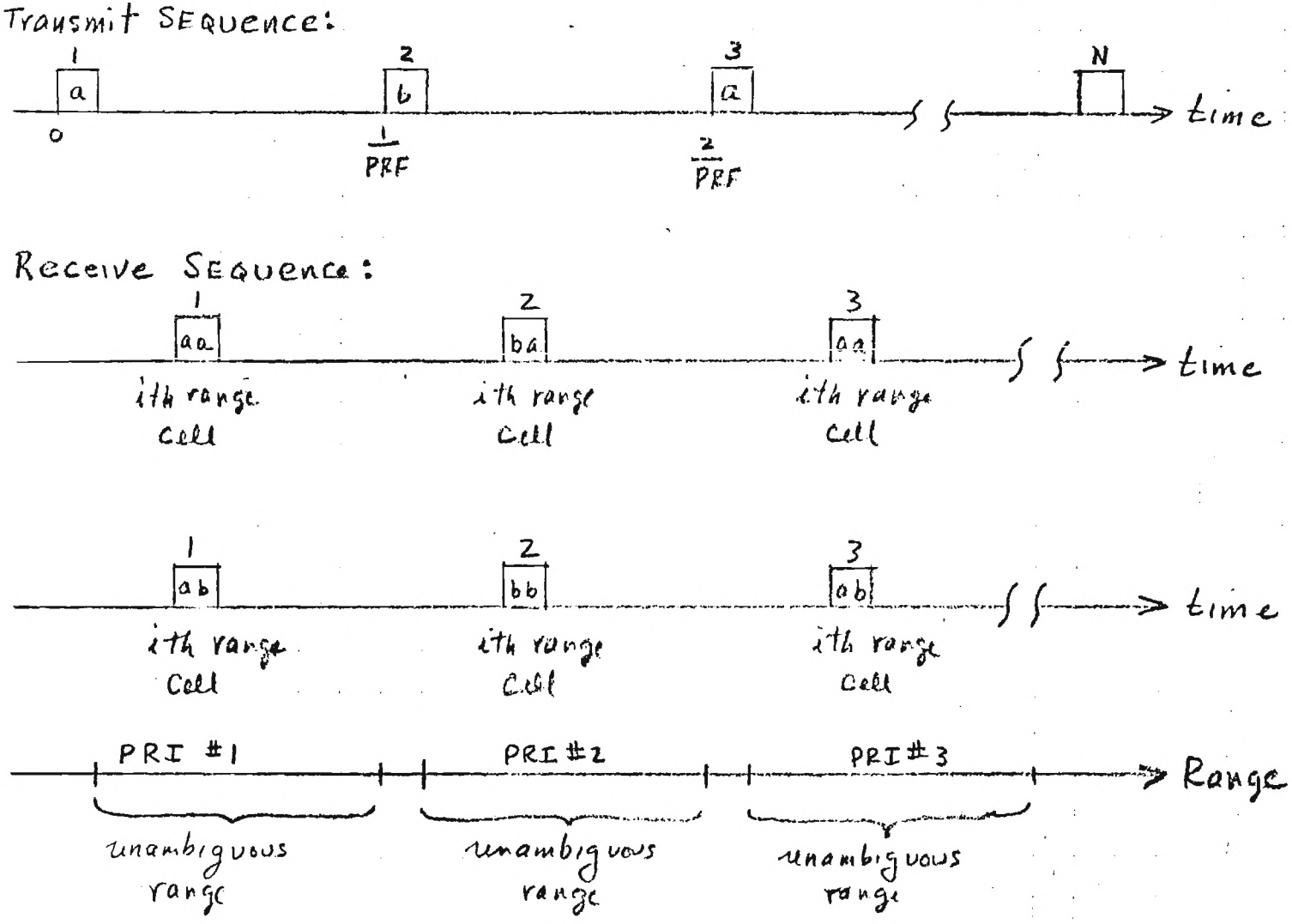

FIGURE 2.

X = a or b orthogonal signals

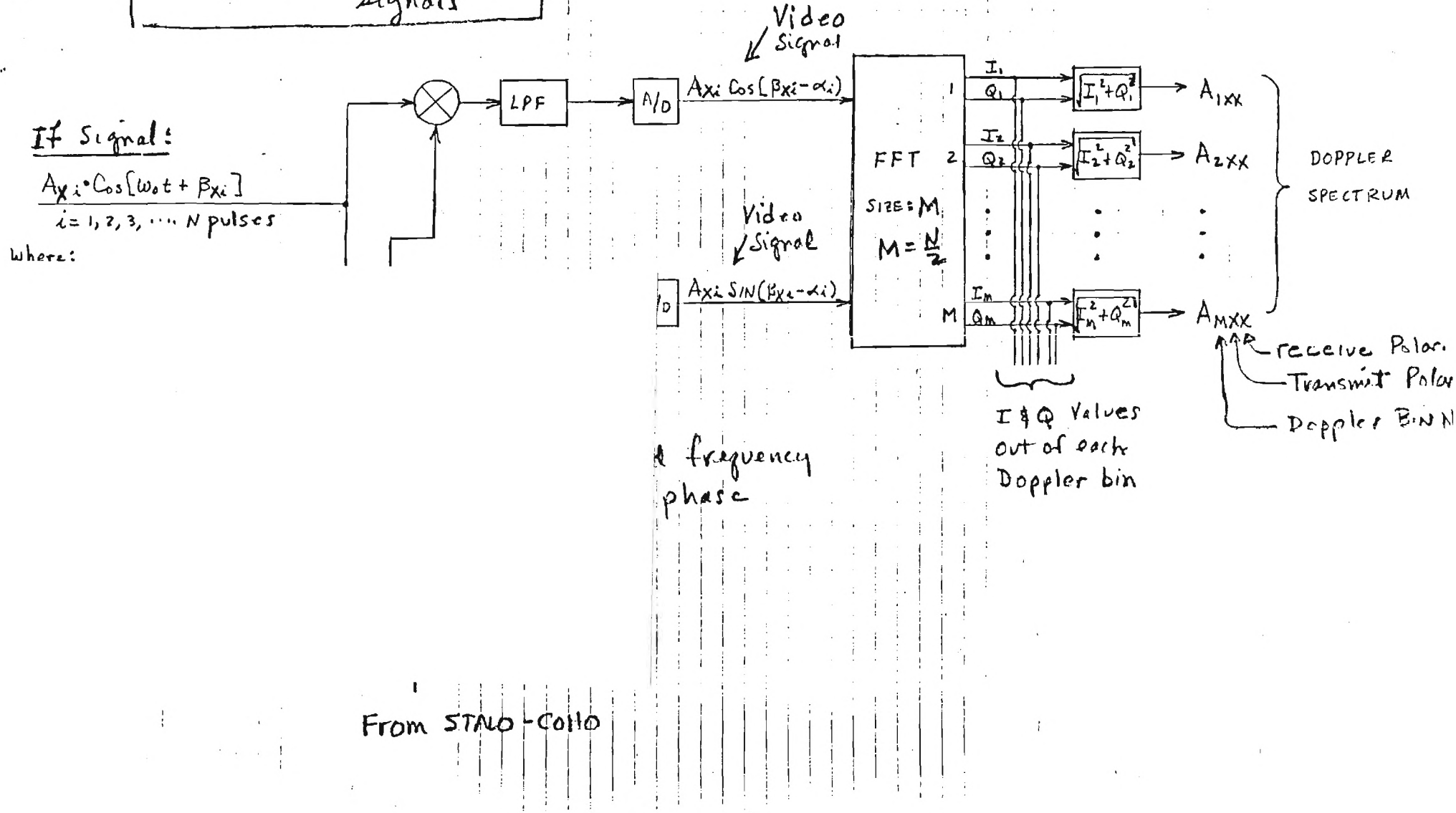

FIGURE 3

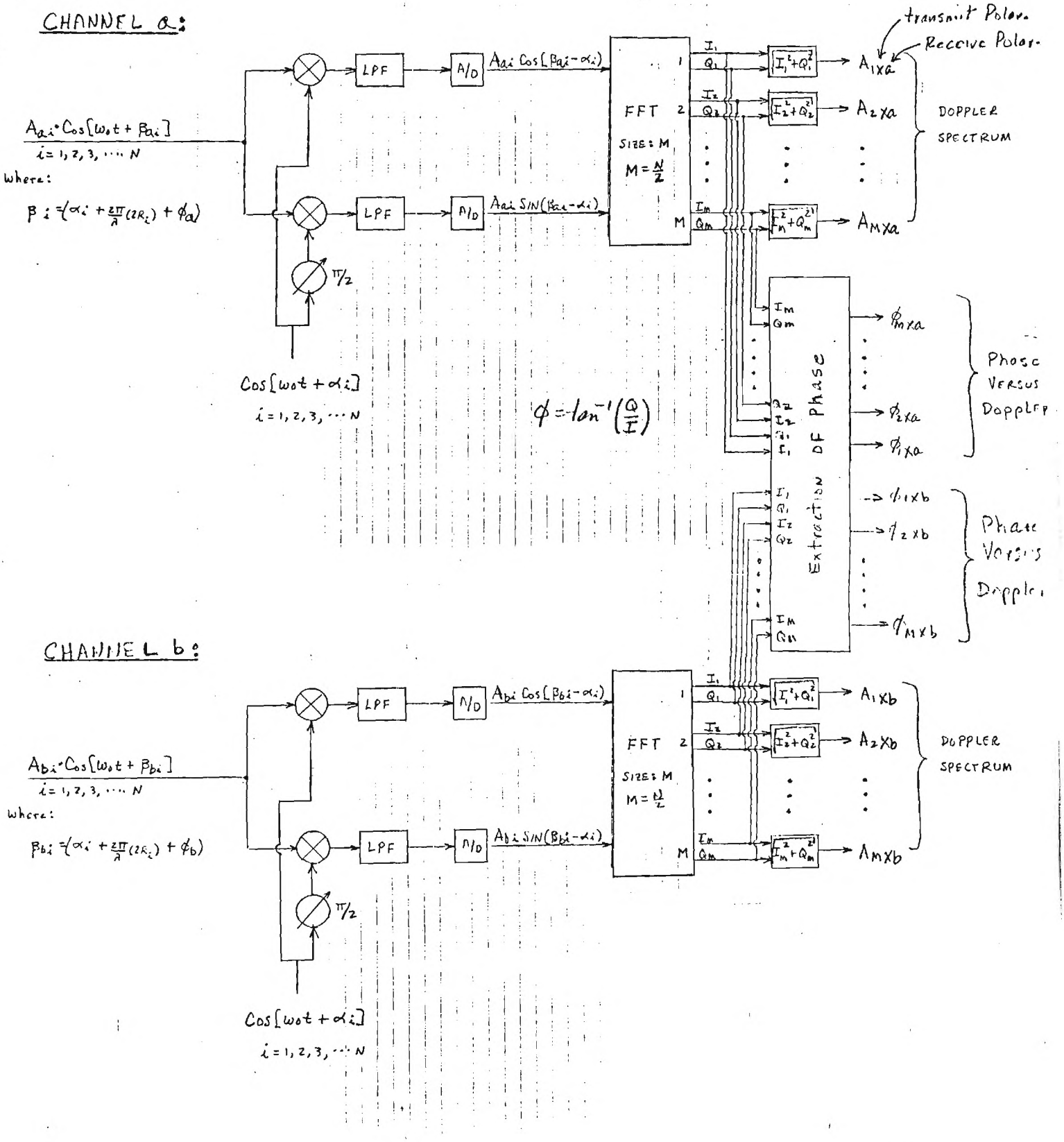
CHANNEL a:
transmit Polar.
Receive Polar.
$A_{ai}\cdot\cos[\omega_o t + \beta_{ai}]$
$i = 1, 2, 3, \cdots N$
Where:
$\beta_i = (\alpha_i + \frac{2\pi}{\lambda}(2R_i) + \phi_a)$
LPF
A/D
$A_{ai}\cos[\beta_{ai} - \alpha_i)$
$A_{ai}\,SIN(\beta_{ai} - \alpha_i)$
FFT
SIZE = M
$M = \frac{N}{2}$
I_1 Q_1 I_2 Q_2 I_m Q_m
$I_1^2+Q_1^2$
$I_2^2+Q_2^2$
$I_m^2+Q_m^2$
A_{1xa}
A_{2xa}
A_{Mxa}
DOPPLER SPECTRUM
$\pi/2$
$\cos[\omega_o t + \alpha_i]$
$i = 1, 2, 3, \cdots N$
$\phi = \tan^{-1}\left(\frac{Q}{I}\right)$
Extraction OF Phase
ϕ_{mxa}
ϕ_{2xa}
ϕ_{1xa}
Phase Versus Doppler
ϕ_{1xb}
ϕ_{2xb}
ϕ_{Mxb}
Phase Versus Doppler
CHANNEL b:
$A_{bi}\cdot\cos[\omega_o t + \beta_{bi}]$
$i = 1, 2, 3, \cdots N$
Where:
$\beta_{bi} = (\alpha_i + \frac{2\pi}{\lambda}(2R_i) + \phi_b)$
LPF
A/D
$A_{bi}\cos[\beta_{bi} - \alpha_i)$
$A_{bi}\,SIN(\beta_{bi} - \alpha_i)$
FFT
SIZE = M
$M = \frac{N}{2}$
I_1 Q_1 I_2 Q_2 I_m Q_m
$I_1^2+Q_1^2$
$I_2^2+Q_2^2$
$I_m^2+Q_m^2$
A_{1xb}
A_{2xb}
A_{Mxb}
DOPPLER SPECTRUM
$\pi/2$
$\cos[\omega_o t + \alpha_i]$
$i = 1, 2, 3, \cdots N$

ENGINEERING EXPERIMENT STATION
Georgia Institute of Technology
A Unit of the University System of Georgia
Atlanta, Georgia 30332

September 23, 1983

Dr. Peter Meischner
DFVLR Oberpfaffenhofen
8031 Wessling

Dear Peter:

This letter report was generated under the provisions of Contract 55312-433X-82. It is a report of the topics discussed by Enterprise Electronics Corporation (EEC), DFVLR, and Georgia Tech, during the three day test plan review held at Georgia Tech on 27, 28, and 29 July. This summary addresses the test that are proposed for the signal processor and the tests proposed for the radar system. We have also included additional comments for your consideration.

A. Design Philosophy

The polarization agile DFVLR Doppler radar is a unique cloud physics data collection system. The precision that can be achieved in maintaining system tolerance determines the resolution of the measurements. Channel isolation, system stability, and signal processor resolution all determine the ultimate system resolution.

The DFVLR staff, in true scientific tradition, will use the this radar to make precision meteorological measurements. The resulting data will be analyzed and ultimately presented to the scientific community. The credibility of the reported meteorological observations will be determined by the precision to which the radar system parameters have been measured and the system stability that can be maintained over long periods of time. The effects of disassembly, transportation, and reassembly of the system will also affect system stability. This report was generated to suggest tests that should be conducted to document system performance and ensure that system design specifications are met.

B. Test Philosophy

Georgia Tech agrees that certain planned EEC test procedures are adequate to test the proper operation of various system modules. We do feel that in general the procedures designed to test the entire system as a unit are inadequate to accurately quantify absolute system performance. For example, tests that utilize the radar's internal coherent local oscillator (COHO), local oscillator (LO), and the proposed software based test routines are acceptable for the purpose of testing primary system

functions. We do feel that EEC should develop test procedures and independent test instrumentation to allow the DFVLR radar performance to be determined as a total stand alone system.

During the test plan review meeting, we requested that a corner reflector array be used to test total system polarization resolution, polarization state repeatability, and polarization stability. If entire system polarization test are not conducted, there will be no way to confirm that the system is meeting the design goal for all polarization states. The use of a corner reflector array is the best way to test total system channel isolation, switch thermal stability (under transmitter radiation conditions), and receiver chain/processor resolution. In addition, dynamic tests should be conducted using a rotating corner reflector to test the receiver and Doppler processing chain. The antenna response should be measured on the antenna range using the raster-scan test to be presented in a later section. Appendix 'A' is a collection of papers that should be useful in quantifying the magnitudes of the effects that you are trying to measure.

C. Signal Processor Dynamic Test

The signal processor design is relatively straight-foward. We recommend that dynamic procedures be used to test the entire system under controled conditions.

The use of a weather balloon lifting a corner reflector was suggested as an independent test of the velocity measurement resolution of the DFVLR radar. A report entitled "Note on Probing Balloon Motion by Doppler Radar" by R. M. Lhermitte is included as Appendix 'B' of this report. The data presented in this report indicate that the balloon is too unstable a platform to test the 1 meter/second velocity resolution of the DFVLR radar.

We therefore suggest that EEC develop a dynamic test proceedure that will employ a moving target of controlled velocity, such as the previously proposed rotating corner reflector. The corner reflector dynamic test will ensure that the receiver/signal processor chain works as a system and that the transmitter and LO have an overall system stability that will allow velocity measurements of 1 meter/second velocity resolution.

Appendix 'C' is a paper entitled "The Correction of I and Q Errors in a Coherent Processor." It is included as a discussion on the errors that can occur in the 'I' and 'Q' channels and the effects of these errors on system accuracy. This paper is included to show the need for measuring Doppler velocity under carefully controled conditions using a rotating corner reflector as outlined in the original Georgia Tech test plan outline. If the EEC test range can not accommodate the rotating corner reflector test, then a condition of system acceptance should be that the velocity test be met at DFVLR using a rotoating corner reflector.

D. Non-Dynamic Tests of the Signal Processor (Tests 3.5, page 5)

a. Acceptable as proposed.

b. Acceptable as proposed.

c. Acceptable as proposed, except maximum switch time should be specified.

d. Same as c.

e. Specifies that the signal processor will output an STC gain control for both linear amplifiers. We suggest that it should be specified that "the gain curves for each amplifier shall be settable independently of each other on a pulse-to-pulse basis."

f. The definition of bandwidth and bandwidth measurement technique should be specified.

g. The power received versus power measured at the IF amplifier should be specified to ensure true log response to within a specified tolerance.

h. The use of a wind-finding radar to make the balloon platform velocity tests (see earlier comments about use of balloon) is not acceptable.

i. Acceptable.

j. Acceptable.

k. We hope that this test will also verify that the correct values appear in the intensity, velocity, and spectral width positions on the display.

E. Test Under Section 3.6.1

a. We agree that weather should not be used to demonstrate that 8 levels can be displayed. This test must be done with a signal generator. The input power levels to the receiver at which each of the 8 levels change should be recorded for test verification purposes.

b. It is unclear how the Doppler data used to test the velocity display will be generated. Could EEC provide more information? The static dihederal corner reflector should be moved in 75 meter range increments to verify that the range resolution is 75 meters.

c. Acceptable as written

d. This test is very important as it establishes the precision to which the system can measure the parameters that make-up the scattering matrix. We support the use of a corner reflector array of the type described in the paper entitled "Passive Polarimetric System" that was distibuted to all attendees during the July meeting. The use of the suggested array has an advantage over a single corner reflector. The array will allow arbitrary polarization components of preselected amplitudes to be generated. The generation of arbitrary polarization components of preselected amplitudes will allow the resolution of the polarization measurement system to be defined.

F. Test Under Section 3.6.3 Phase Stability

a. This paragraph states that the minimum Doppler resolution is only 2.55 meters per second if the promised 7 degree phase stability specification is met. The footnote (asterisks) stating that "This does not imply that the point target

velocity accuracy will be worse than 1 meter per second" is very confusing. We do not fully understand this statement. Could EEC or DFVLR clarify?

G. Test Under Section 6.0 Signal and Data Processing Subsystems

We have no written specification for the digital signal simulator that will be used to test the signal processor. It would be advisable to request a set of specifications from EEC concerning the digital signal simulator design. Hopefully, the digital signal simulator is a stand alone system. We do not think that the stable local oscillator or coherent local oscillator in the DFVLR radar should be used to simulate any signals for absolute test, as the use of system components are acceptable only for testing system modules.

H. General Pulse Pair Processor Algorithm.

Georgia Tech does not have a detailed description of the DFVLR signal processor. We do have the manual supplied by Sigmet that discusses how the mean Dopper velocity is computed and how the elements of the scattering matrix are computed, in general terms. We have therefore located a number of papers on pulse pair processing (PPP) the scattering matrix calculations and, using these papers, we have developed a simplified algorithm that explains the PPP technique. We have included several of these papers on the PPP technique as Appendix 'D' for your use and study.

1. Computation of Mean Doppler Velocity

The DFVLR radar is designed to provide a mean Doppler estimate and a velocity variance estimate for each of 2 channels for each of 2 polarization states. Figure 1 shows the convention that will be used to describe the data channels.

When 'I' is shown, the inphase channel is referenced. The term 'Q' refers to the quadrature channel. There are 2 'I' and 2 'Q' channels processed for each polarization state. The raised 'xx', 'xy', 'yy', and 'yx' indicate polarization states. The first letter in the group indicates the transmitted polarization and the second letter indicates the received polarization. In the case of Figure 1, 'xx' indicates transmit 'x' polarization and receive 'x' polarization, while 'xy' indicates transmitt 'x' polarization and receive 'y' polarization. The designator '1' indicates the pulse number. The transmitter always transmits in the 'X' channel on the odd pulses (1,3,5,7,9.....N).

Figure 2 shows a similar convention, except the polarization has been switched to the orthogonial state. The transmitter is now transmitting in the 'Y' channel. The pulse number is '2'. The transmitter will transmitt in the 'Y' channel on all even pulses (2,4,6,8,10.....N). The raised subscript changes to 'yy' or 'yx' to show this fact.

Figure 3 shows how the combination of values, shown in Figures 1 and 2, are generated. There are two linear intermediate frequency (IF) amplifiers; one for the 'X' channel and one for the 'Y' channel. The gain of each should be capable of being set separatly. The output of either 30 MHz linear IF amplifier feeds the input port of a non-limiting phase detector. The 30 MHz output of the COHO feeds the other port of the non-limiting phase detector. The resulting output of the phase detector is an in-phase (I) channel and the quadrature (Q) channel. Since there are two IF amplifiers there are two 'I' and two 'Q' channels to be processed for each polarization state.

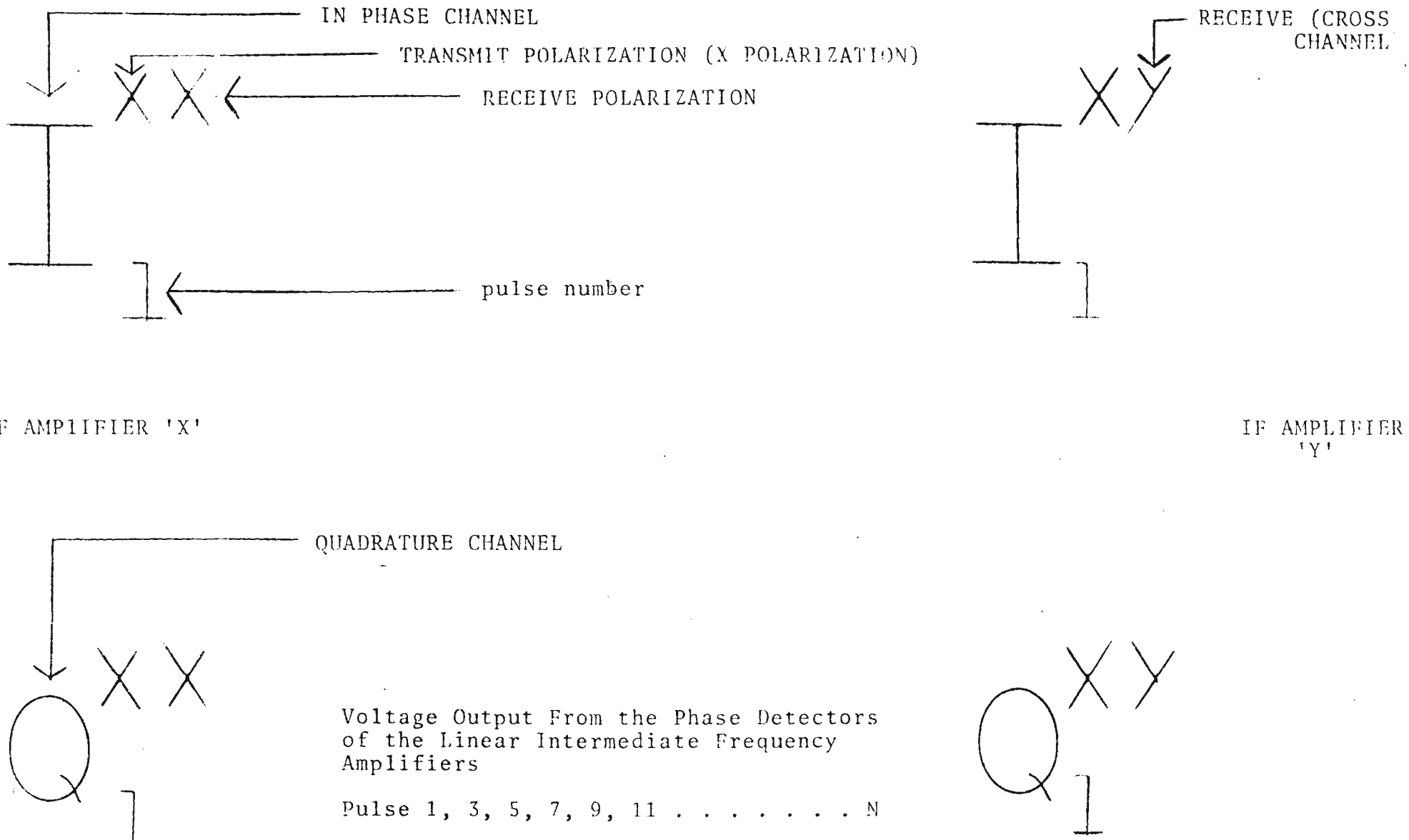

Figure 1. Polarization Channel Coding Scheme Pulse Number 1.

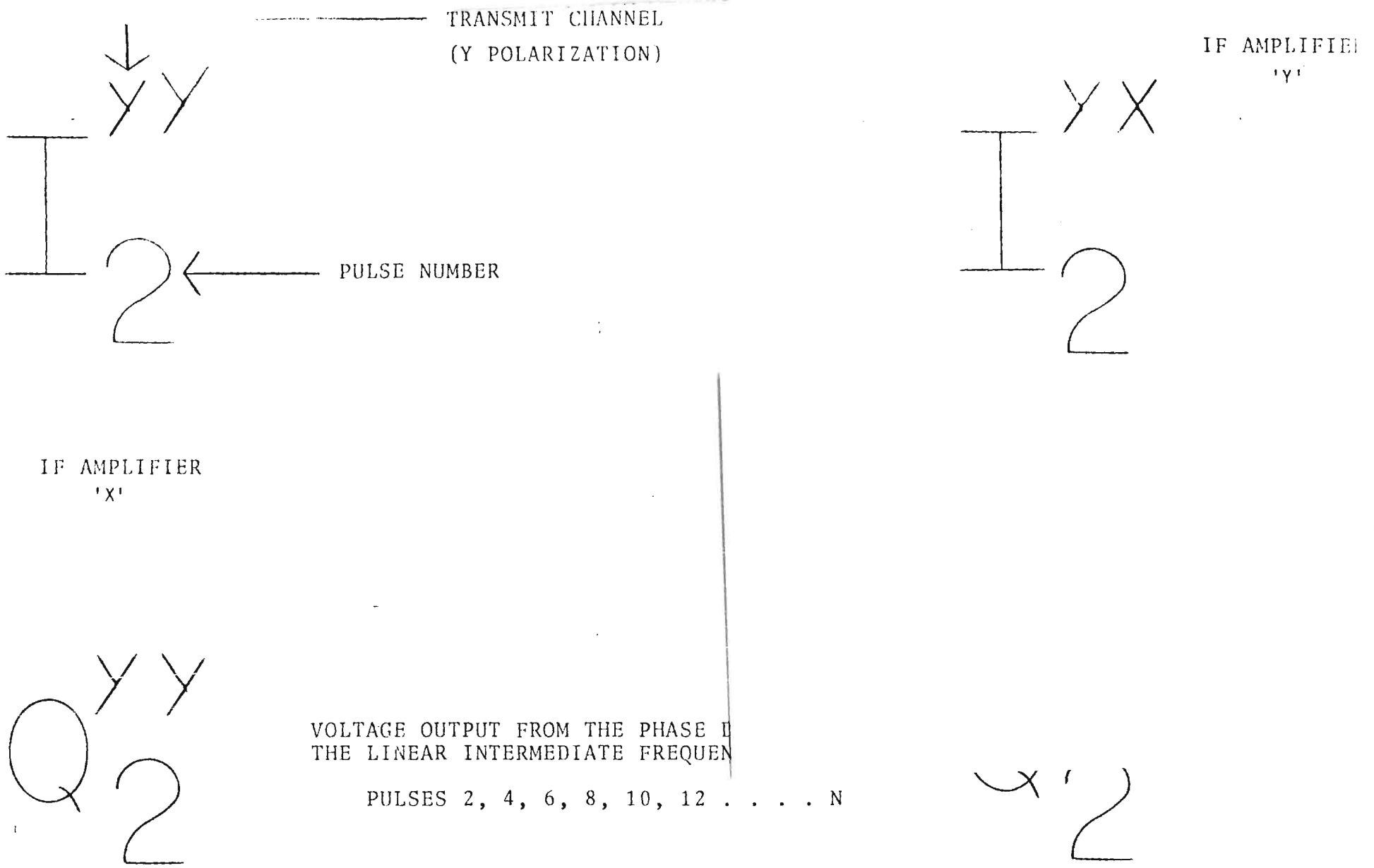

Figure 2. Polarization channel coding scheme pulse 2.

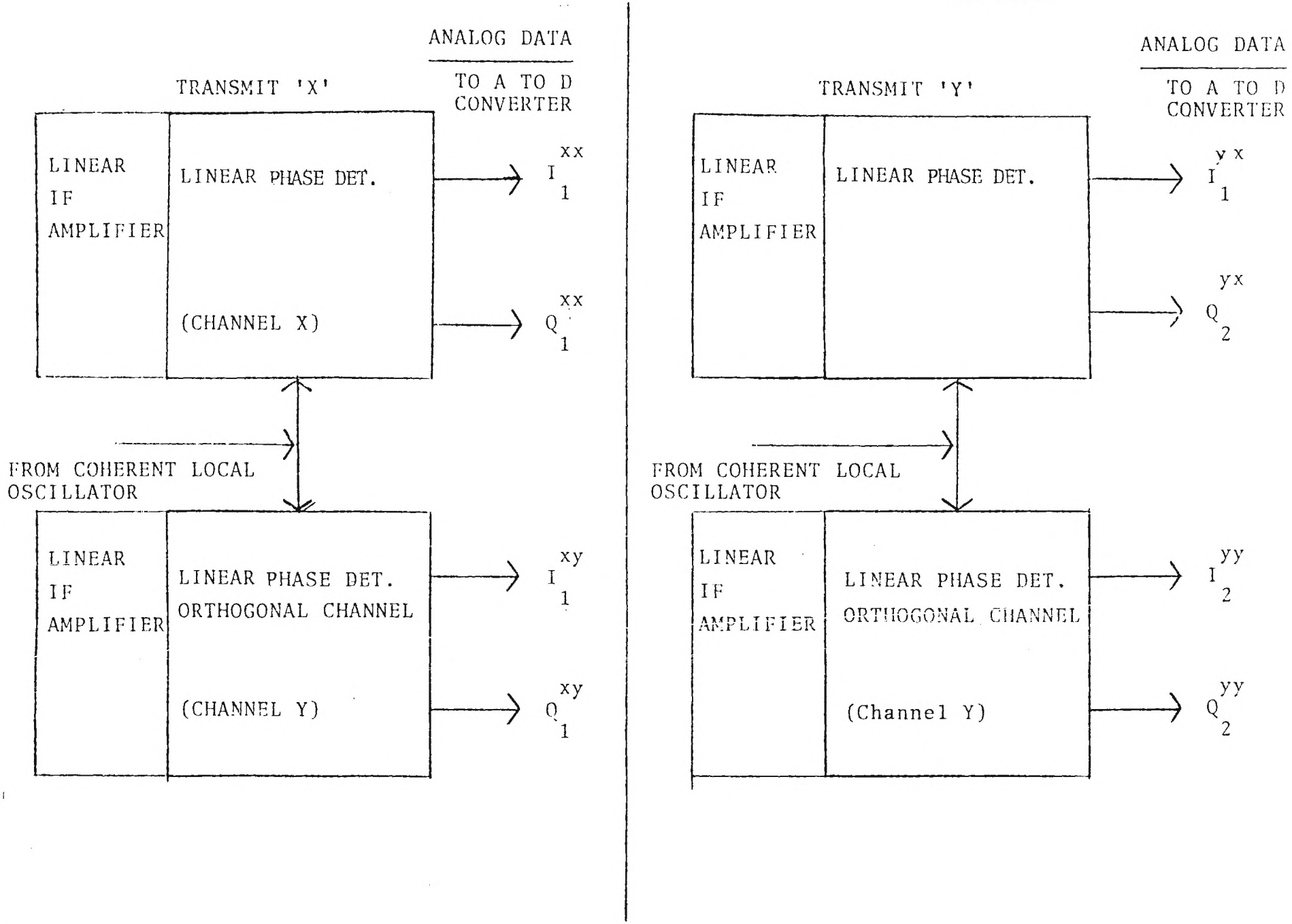

Figure 3. Linear amplifier and phase detector output.

Pulse 1 is transmitted in the 'X' channel and 4 analogue values (I^{xx}, Q^{xx}, I^{xy}, Q^{xy}) are digitized by the 10 bit analogue to digital converter. The polarization state is switched and pulse 2 is transmitted in the 'Y' orthogonal channel. The next 4 additional analogue values (I^{yy}, Q^{yy}, I^{yx}, Q^{yx}) are digitized by the 10 bit analogue to digital converter. These values are stored in an even integer pulse number location.

Figure 4 shows a typical data storage scheme. The pulse numbers are shown across the top. The transmit polarization is shown along the left margin. The data collected for pulse numbers 1 through 6 are shown, as are the data for pulse numbers 13 and 14. In actual practice 32, 64, or 128 pulses will be collected at one time and stored as shown.

The storage scheme shown in Figure 4 shows how the pulses will be processed by the pulse pair processor. Refering to the illustration shown in Figure 4, pulses 1 and 3 will be treated as a pair and pulses 2 and 4 will be treated as a pair. Pulses 3 and 5 will be treated as a pair and pulse 4 and 6 will be treated as a pair. Pairs of 'I' and 'Q' values are processed in the order shown because the polarization is switched on each pulse, and each pair processed must come from the same polarization state.

The terms 'Imag' and 'Real' are computed from the 'I' and 'Q' values developed in Figure 4. The variable names 'Real' and 'Imag' are assigned to the sum and difference of the terms in the numerator and denominator of the series shown in Figure 5 as step (1). The values for 'Real' and 'Imag' are computed for any 32, 64, or 128 pulses from a specific polarization, in this case polarization state 'xx'.

The 'I' and 'Q' values are ordered as shown in Step 1, Figure 4 and the mathematical operations shown are performed. The terms in the series would be expanded to 32, 64, or 128 samples in a complete example. When the indicated mathematical procedures are performed, the 'Real' and 'Imag' variables are assigned the computed values. The 'Real' and 'Imag' values will have a plus '+' or minus '-' sign, depending on their value. The sign information for the 'Real' and 'Imag' values is saved in step (3) for use in step (6). The value of the intermediate variable 'Uxx' is computed in step (4) by dividing the 'Imagxx' value by the 'Realxx' value.

Figure 6 shows how the mean Doppler angle is computed. The average angular step between pulse pairs, shown as ϕxx, is computed over the interval of 32, 64, or 128 pulses and is found in step (5) by taking the arctangent of 'Uxx'.

The calculated average value of ϕxx lies between 0 and $2/\pi$ radians at this point in the calculation. The true value can lie between $-\pi$ and π radians. The signs that were saved during step (3) of Figure 5 are used to resolve this ambiguity.

A truth table was constructed in step (6) to determine the angle to add to ϕxx to find the true average angle $\overline{\phi xx}$. If the sign of 'Realxx' and 'Imagxx' are both '+', then the value of ϕxx is the correct value of $\overline{\phi xx}$. If the sign of 'Imagxx' is '-' and the sign of 'Realxx' is '+', then $\overline{\phi xx}$ is equal to $\phi xx - \pi$. If the signs of both 'Imagxx' and 'Realxx' are '-', then $\overline{\phi xx}$ equals $\pi - \phi xx$. If the sign of 'Imagxx' is '+' and the sign of 'Realxx' is '-', then the value of $\overline{\phi xx}$ is $2\pi - \phi xx$.

When the value of $\overline{\phi xx}$ has been determined, the mean Doppler 'Fdxx' can be calculated. This calculation is shown in step (7). The pulse repetition frequency (PRF) is divided by 4π instead of the normally used 2π because of the order in which the pulse pairs were collected. The polarization state is switched on every other pulse (i.e., pulses

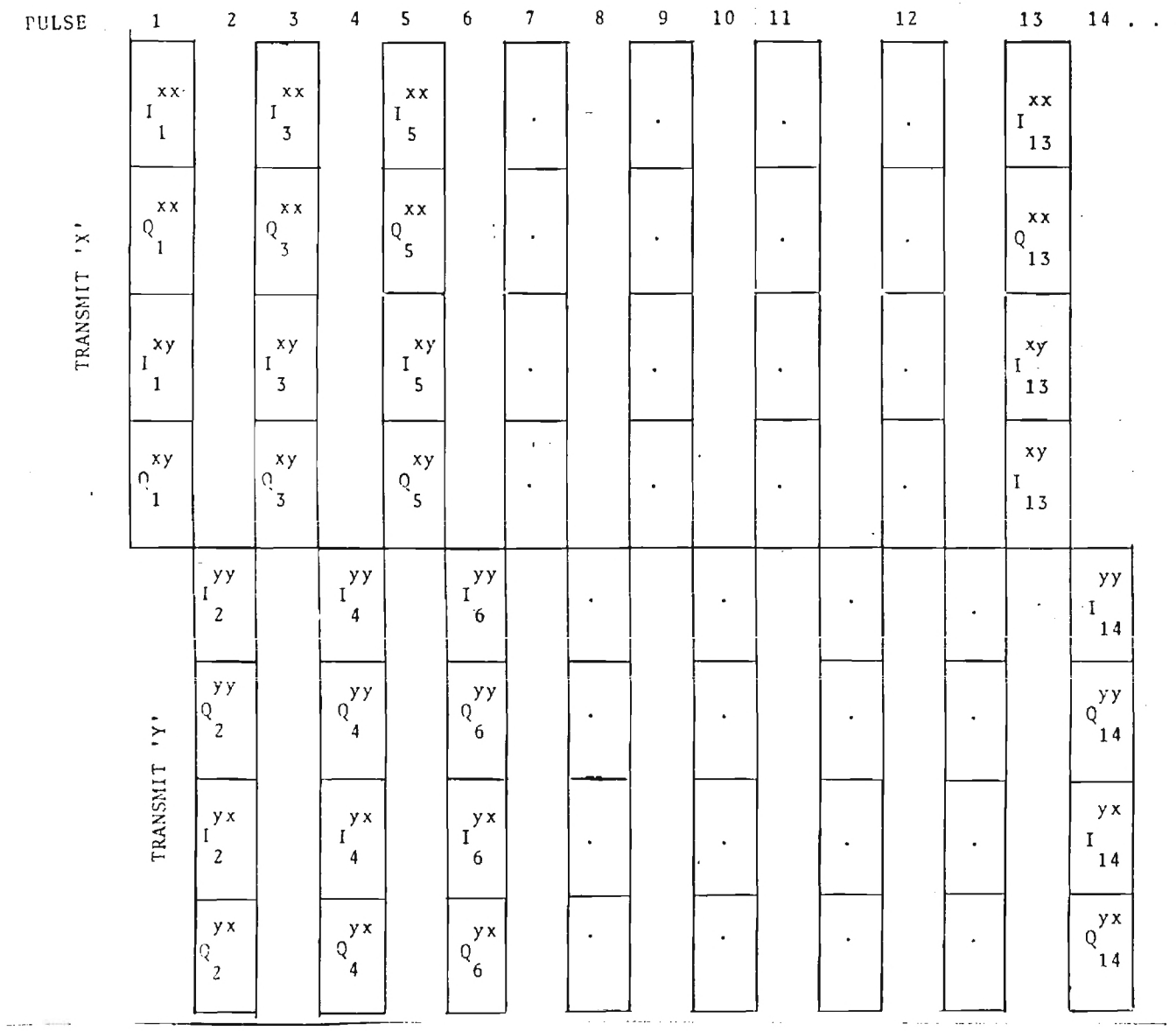

Figure 4. Typical way that data is stored by pulse number.

COMPUTATION OF MEAN DOPPLER FREQUENCY FOR XX
(REPEAT SAME STEP FOR XY, YY, AND YX VALUES)

Transmit = xx

Receive = xx

I^{xx} AND Q^{xx}

S $\quad Imag_{xx} = \left[\left(I_1^{xx} \cdot Q_3^{xx} \right) - \left(I_3^{xx} \cdot Q_1^{xx} \right) + \left(I_3^{xx} \cdot Q_5^{xx} \right) - \left(I_5^{xx} \cdot Q_3^{xx} \right) + \left(I_5^{xx} \cdot Q_7^{xx} \right) \ldots N \right]$ (1)

S $\quad Real_{xx} = \left[\left(I_3^{xx} \cdot I_1^{xx} \right) + \left(Q_3^{xx} \cdot Q_1^{xx} \right) + \left(I_5^{xx} \cdot I_3^{xx} \right) + \left(Q_5^{xx} \cdot Q_3^{xx} \right) + \left(I_7^{xx} \cdot I_5^{xx} \right) \ldots N \right]$ (2)

(3) STORE SIGNS OF $Imag_{xx}$ & $Real_{xx}$ (4) COMPUTE V_{xx}

$$v_{xx} = \frac{Imag_{xx}}{Real_{xx}}$$

SAVE SIGN FOR QUADRANT TEST

SAVE SIGN FOR QUADRANT TEST

Figure 5. Computation of mean Doppler frequency.

(5) COMPUTE AVERAGE (ϕ)

$$\phi_{xx} = \text{TAN}^{-1} (\nu_{xx})$$

(6) COMPUTATION OF $\overline{\phi_{xx}}$

TRUTH TABLE

Imag_{xx}	Real_{xx}	$\overline{\phi_{xx}}$
+	+	$\phi_{xx} = \overline{\phi_{xx}}$
-	+	$\phi_{xx} - \pi = \overline{\phi_{xx}}$
-	-	$\pi - \phi_{xx} = \overline{\phi_{xx}}$
+	-	$2\pi - \phi_{xx} = \overline{\phi_{xx}}$

(7) COMPUTE MEAN DOPPLER FREQUENCY ($f_{d_{xx}}$)

$$f_{d_{xx}} = \frac{PRF}{4\pi} \cdot (\overline{\phi_{xx}})$$

STEP 8 - 21

Compute f_d for xy, yy, and yx using same algorithm as steps 1 - 7 and changing case for polarization.

(22) SAVE VALUES

$f_{d_{xx}}$, $f_{d_{xy}}$, $f_{d_{yy}}$, and $f_{d_{yx}}$

Figure 6. Computation of mean Doppler frequency.

COMPUTATION OF VARIANCE OF XX CASE

(1) COMPUTE VALUE OF V_{xx}

$$V_{xx} = \left[\frac{\left(\left(\begin{matrix} xx & xx \\ I_1 & I_3 \end{matrix} \right) + \left(\begin{matrix} xx & xx \\ Q_1 & Q_3 \end{matrix} \right) + \left(\begin{matrix} xx & xx \\ I_3 & I_5 \end{matrix} \right) \cdots N \right)^2}{\left(\left(\begin{matrix} xx & xx \\ I_1 & I_5 \end{matrix} \right) + \left(\begin{matrix} xx & xx \\ Q_1 & Q_5 \end{matrix} \right) + \left(\begin{matrix} xx & xx \\ I_3 & I_7 \end{matrix} \right) + \left(\begin{matrix} xx & xx \\ Q_3 & Q_7 \end{matrix} \right) \cdots N \right)^2} + \right.$$

$$\left. \frac{\left(\left(\begin{matrix} xx & xx \\ I_3 & Q_1 \end{matrix} \right) - \left(\begin{matrix} xx & xx \\ I_1 & Q_3 \end{matrix} \right) + \left(\begin{matrix} xx & xx \\ I_5 & Q_3 \end{matrix} \right) - \left(\begin{matrix} xx & xx \\ I_3 & Q_5 \end{matrix} \right) \cdots N \right)^2}{\left(\left(\begin{matrix} xx & xx \\ I_5 & Q_1 \end{matrix} \right) - \left(\begin{matrix} xx & xx \\ I_1 & Q_5 \end{matrix} \right) + \left(\begin{matrix} xx & xx \\ I_7 & Q_3 \end{matrix} \right) - \left(\begin{matrix} xx & xx \\ I_3 & Q_7 \end{matrix} \right) \cdots N \right)^2} \right]^{1/2}$$

(2) COMPUTE VARIANCE (σ_{xx})

$$\sigma_{xx} = \frac{\sqrt{\frac{2}{3} \cdot \ln \cdot V_{xx}}}{(2\pi)^2} \cdot \frac{(PRF)^2}{4}$$

-OR-

$$\sigma_{xx}^2 = \sqrt{\sigma_{xx}}$$

STEPS 3 - 8

Compute σ_{xx} for xy, yy, and yx using same algorithm and changing case for polarization

(9) SOLVED VALUES

xx' xy' yy' and yx

Figure 7. Computation of variance.

1,3,5.....N are paired and pulses 2,4,6,....N are paired). The value of PRF/4π then is multiplied by ϕxx, producing the value of the mean Doppler frequency, fdxx, which is in units of Hertz.

This same procedure is repeated in steps (8) through (21) for the computation of the mean Doppler for the terms fdxy, fdyy, and fdyx. The mean Doppler values for these terms are stored in step (22). The variance or Doppler spread of each of the 4 mean Doppler terms must be computed.

2. Computation of Doppler Variance

Figure 7 shows how the Doppler variance is computed for the 'xx' case. The 'I" and 'Q' values are grouped as shown in step (1) of Figure 7. The indicated mathematical operations are performed and a value is assigned to variable 'Vxx'. Step (2) is performed according to Sigmet documentation. The square root of the terms under the radical is taken. The result is the variance (σxx). The variance is a measure of spectrum width which serves as an indicator of the velocity spectrum of all hydrometeors in the radar range/azimuth cell of interest. The velocity spectrum serves as a measure of the size distribution of the hydrometeors in the beam.

3. Computation of the Scattering Matrix

This section is in preparation and will be forwarded in the near future. We did not want to hold this report until the scattering matrix explanation is complete.

The section that follows this part of the report contains comments prepared by Mr. J. S. Ussailis. The points made in his attached report are the same points made during the DFVLR/EEC/Georgia Tech meeting in July.

If there are questions please feel free to call me. The scattering matrix information will be forwarded upon completion.

Yours Truly,

Gene Greneker
Project Director

A-3383

ENGINEERING EXPERIMENT STATION
Georgia Institute of Technology
A Unit of the University System of Georgia
Atlanta, Georgia 30332

December 19, 1983

Dr. Peter Meischner
DFVLR Oberpfaffenhofen
8031 Wessling

Dear Peter:

This letter is in response to your request for an explanation of how EEC proposes to compute the elements of the scattering matrix and also to clarify a mistake that we made in the explanation of how the mean Doppler variance is computed.

A. The EEC Method of Computing Variance

Our last letter included a section showing how the mean Doppler velocity and the variance of the mean Doppler velocity were computed, using 'I' and 'Q' values. The method of computing the mean Doppler frequency is correct as presented. The method of computing the variance is also correct; however, the method presented by Georgia Tech is not the method used by EEC to compute the variance of the mean Doppler frequency.

Figure 1 shows the process used by EEC to compute the variance of the mean Doppler frequency. This method uses 7 steps in the computation. The digitized 'I' and 'Q' values are stored in the primary data array (shown as figure 4 in the November report). A 32, 64, or 128 point Fast Fourier Transform (FFT) is performed on the 'I' and 'Q' values in step 2. The output of the FFT is the voltage spectrum. An algorithm to remove the ground clutter is performed in step 3. This involves the removal of spectral components that lie around the zero velocity line of the spectrum. The components that lie near the zero velocity line represent the spectral components contributed to the spectrum by ground clutter. The 'real' and 'imaginary' spectral values, produced by the FFT, are squared in step 4. The inverse FFT is then performed on the 'real' values and the 'imaginary' array is loaded with zero values. The squared frequency spectrum valves are then transformed back to the time domain. The second and third points (Point 1 represents zeroth lag) of the transformed time series represent the first and second lags (R1 and R2).

The variance is computed by taking two thirds of the natural log of the ratio of the absolute value of the first and second lags (R1 and R2) as shown in step 6 and performing the operation shown in Step 7. According to EEC, the resulting value is the variance. The standard deviation may be computed (if desired) by taking the square root of the variance.

B. Computation of the Scattering Matrix Elements

The 'I' and 'Q' values are collected and stored as shown in figure 4 of the November report. The first step in computing the elements of the scattering matrix is the computation of the amplitude values $\overline{S^{xx}}$, $\overline{S^{xy}}$, $\overline{S^{yx}}$, and $\overline{S^{yy}}$. As shown in step 1 of figure 2, the value of $\overline{S^{xx}}$ is computed by squaring the 'I' and 'Q' values, performing the indicated multiplication, and then summing the results over the odd pulses pairs. The value of $\overline{S^{xy}}$ is computed the same way, by also using pulses 1, 3, 5, 7.....N-1. The

amplitude of $\overline{S^{xy}}$ and $\overline{S^{yy}}$ are computed in the same way, except pulses 2, 4, 6, 8.....N are used in the computation.

Step 2 shows the elements of the phase term $\overline{\phi^{xy}}$, and the general equation supplied by EEC is shown. The 'I' and 'Q' variables are substituted in the equation in step 3. The 'I' and 'Q' terms are multiplied in step 4, and 'j' (the imaginary term) is removed from one set of terms through algebraic manipulation, resulting in a sign change. The sums of the imaginary and real values are taken in step 5, and their signs are saved in step 6. These signs will be used to solve the inverse tangent ambiguity (in step 9).

The ratio of the real and imaginary values is taken in step 7 and the resulting value is assigned to the variable V^{xy}. The mean phase angle ϕ^{xy} is computed in step 8 by taking the inverse tangent of variable V^{xy}. The possible quandrant ambiguity in the phase angle of ϕ^{xy} is corrected in step 9 by testing the stored signs of the real and imaginary values (those stored in step 6). The phase angle $\overline{\phi^{xy}}$ is the corrected mean phase angle that will be used in the scattering matrix.

The calculation of $\overline{\phi^{yx}}$ is accomplished in step 10 by using the same procedure outlined in steps 2 through 9 with one exception. The 'I' and 'Q' values used to calculate $\overline{\phi^{yx}}$ come from the even pulse group. Therefore the pulse number of the 'I' and 'Q' values will run from 2 to 32 instead of 1 to 31, as in the previous example.

The phase angle $\overline{\phi^{yy}}$ is computed starting with step 11. The general form of the equation used in this calculation is shown in step 11, and the general equation with substituted 'I' and 'Q' values are shown in step 12. The 'I' and 'Q' values are taken from both the odd and even pulses in the calculation of $\overline{\phi^{yy}}$. The 'I' and 'Q' values are grouped as shown in step 13 and the 'j' term is removed algebraically. The sums of the real and imaginary terms are taken in step 14 using all 32 samples in the order shown. The signs are stored in step 15 for use in step 18. The ratio of the real and imaginary values is

taken in step 16 and assigned to the variable V^{yy}. The phase angle ϕ^{yy} is computed in step 17 by taking the inverse tangent of variable V^{yy}. The quandrant ambiguity is removed in step 18 by use of the truth table. The unambigious phase angle $\overline{\phi^{yy}}$ can now be used in the scattering matrix. Step 19 shows that after the computation and correction of $\overline{\phi^{xx}}$ there are 3 phase angles for use in the scattering matrix.

The general form of the EEC scattering matrix is shown in step 20. There are 4 signal amplitude values $\overline{S^{xx}}$, $\overline{S^{xy}}$, $\overline{S^{yx}}$, and $\overline{S^{yy}}$ and three phase values. The phase value $\overline{\phi^{xx}}$ has been subtracted from each phase term in the matrix. The subtraction process of $\overline{\phi^{xx}}$ sets the phase term associated with S^{xx}'s to zero. The term $\bar{\theta}$ is computed in a two step process in sps 21 and 22.

The mean Doppler frequency fd_{yy} and fd_{xx} computed by the pulse pair processor (shown in the November report) are recalled and averaged in step 21. This averaging produces variable $\overline{f_d}$, which represents the average Doppler frequency of the two mean Doppler frequency estimates fd_{yy} and fd_{xx}. The mean phase angle $\bar{\theta}$, is computed using the averaged Doppler velocity, $\overline{f_d}$ computed in step 21. The mean Doppler frequency is converted to phase angle $\bar{\theta}$ (in units of radians) in step 22 in order to have units that are equivalent to the phase terms in the scattering matrix.

The elements of the scattering matrix, as defined by EEC, are shown in step 23. The phase term associated with amplitude term $\overline{S^{xx}}$ is set to zero. The phase term associated with amplitude term $\overline{S^{xy}}$ is shown as $\overline{\phi^{xy}}$. The phase term associated with $\overline{S^{yx}}$ is the sum of phase angles $\overline{\phi^{yx}}$ and $\overline{\phi^{yy}}$, minus the phase angle $\overline{\theta/2}$. The phase term associated with amplitude term $\overline{S^{yy}}$ is $\overline{\phi^{yy}}$ minus $\overline{\theta/2}$.

The term $\bar{\theta}$ must be subtracted from 2 elements in the matrix to remove all contribution of phase shift between channels due to Doppler induced phase shift.

Ideally, all amplitude and phase terms in the matrix would be taken during a single pulse. However, these terms are generated over successive pulse pairs by switching polarization in the EEC/DFVLR radar. Therefore, twice the Doppler phase appears in the phase terms in the scattering matrix and must be removed before the polarimetric phase can be determined. The removal of the Doppler phase term theoretically removes all non-polarimetric phase information, except the polarimetric phase between channels due to effects of the medium. After the Doppler phase term has been removed, the polarmetric phase can be resolved to a high degree of accuracy for a single point target, using this technique. We suspect that spectral broadening (due to multiple velocities being present in a rainfall distribution) will degrade the cancellation of the Doppler phase term, and this may prohibit using the scattering matrix, as presently derived, to observe small polarimetric phase shifts on the order of 5^{o}.

C. Questions about the EEC processing Technique

The term $\overline{\theta/2}$ appears in the scattering matrix. It is EEC's contention that the reason that $\overline{\theta}$ is divided by 2 is because $\overline{\theta}$ is computed over two pulse pairs and therefore the equivalent mean Doppler angle is twice its proper value. We believe that $\overline{\theta}$ should not be divided by 2 because the phase angle represented by $\overline{\theta}$ is the correct mean Doppler frequency. Perhaps we do not fully understand the processing procedure, but this would be a good point to check with EEC.

If there are questions regarding this explanation please let me know.

Yours truly,

Gene Greneker III

cc: EKR, JLE, NCC, JDE, YMP, Pat Heitmuller

(1) 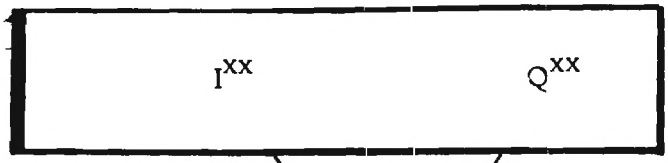

Collect 'I' and 'Q' values

(2) 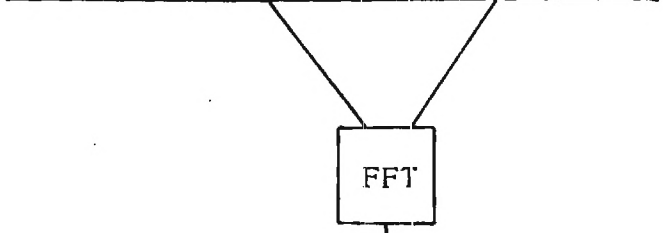

Perform FFT on 'I' and 'Q' valves and compute a Voltage spectrum

(3) 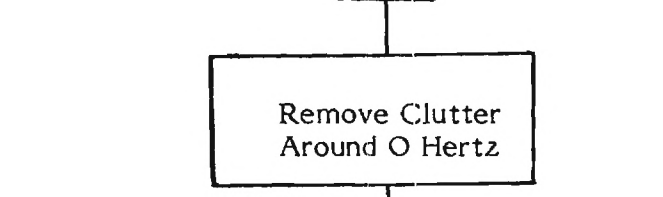

Remove the frequencies that lie around zero velocity bin. These low frequencies represent clutter.

(4) 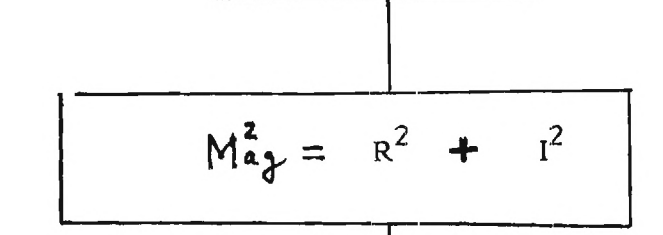

Square the 'Real' and 'Imaginary' values that represent the Voltage Spectrum.

(5) 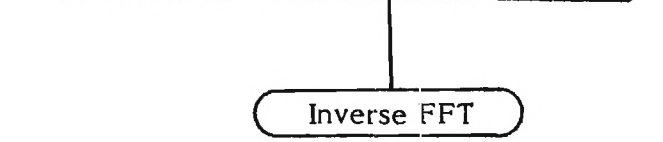

Perform the inverse FFT on the squared 'Real' and 'Imaginary' Values

(6) $$V = \frac{2}{3} \times LN \left(\left| \frac{R_1}{R_2} \right| \right)$$

Take two thirds the natural log of the ratio of LAG 1 (R1) and LAG 2 (R2), which are the first 2 points of the inverse transform.

(7) $$\sigma^2 = \frac{V}{(2\pi)^2} \times (PRF)^2$$

This Produces the Variance.

$$\text{Std dev} = \sqrt{\sigma^2}$$

The standard deviation provides the 1 sigma spectrum spread

Figure 1. Method used by EEC to compute variance

Step 1. Computation of $\overline{S^{xx}}$, $\overline{S^{xy}}$, $\overline{S^{yx}}$, $\overline{S^{yy}}$

$$\overline{S^{xx}} = (I_1^{xx})^2 \times (Q_1^{xx})^2 + (I_3^{xx})^2 \times (Q_3^{xx})^2 + \ldots\ldots (I_{31}^{xx})^2 \times (Q_{31}^{xx})^2$$

$$\overline{S^{xy}} = (I_1^{xy})^2 \times (Q_1^{xy})^2 + (I_3^{xy})^2 \times (Q_3^{xy})^2 + \ldots\ldots (I_{31}^{xy})^2 \times (Q_{31}^{xy})^2$$

$$\overline{S^{yx}} = (I_2^{yx})^2 \times (Q_2^{yx})^2 + (I_4^{yx})^2 \times (Q_4^{yx})^2 + \ldots\ldots (I_{32}^{yx})^2 \times (Q_{32}^{yx})^2$$

$$\overline{S^{yy}} = (I_2^{yy})^2 \times (Q_2^{yy})^2 + (I_4^{yy})^2 \times (Q_4^{yy})^2 + \ldots\ldots (I_{32}^{yy})^2 \times (Q_{32}^{yy})^2$$

32 PULSES

Figure 2. Computation of Scattering Matrix

(2) Elements that comprise the equation for the solution of $\overline{\phi^{xy}}$

$$\overline{\phi^{xy}} \triangleq \text{Arg}\left(\sum_{i = 1, 3, 5 \ldots\ldots N-1} A_i^{xy} \cdot (A_i^{xx})^*\right)$$

(3) Substitution of mathematical operators and 'I' and 'Q' Values

$$\overline{\phi^{xy}} \triangleq \text{Arg}\left(\sum_{i = 1, 3, 5\ldots\ldots N-1} (I_i^{xy} + jQ_i^{xy}) \cdot (I_i^{xx} - jQ_i^{xx})\right)$$

(4) Multiplication and collection of I^{xx}, I^{xy}, Q^{xx} and Q^{xy} terms.

$$(I_i^{xy} \times I_i^{xx}) + (jQ_i^{xy} \times I_i^{xx}) - (jQ_i^{xy} \times jQ_i^{xx}) - (I_i^{xy} \times jQ^{xx})$$

$$+ (Q_i^{xy} \times Q_i^{xx})$$

$$(I_i^{xy} \times I_i^{xx}) + (jQ_i^{xy} \times I_i^{xx}) + (Q_i^{xy} \times Q_i^{xx}) - (I_i^{xy} - jQ^{xx})$$

(5) Sum the real and imaginary terms using 16 odd numbered pulses from the 32 pulses transmitted using the relationship:

$$/S/\ \text{IMAG} = (Q_1^{xy} \times I_1^{xx}) - (I_1^{xy} \times Q_1^{xx}) + (Q_3^{xy} \times I_3^{xx}) - (I_3^{xy} \times Q_3^{xx})$$

$$\ldots\ldots (Q_{31}^{xy} \times I_{31}^{xx}) + (I_{31}^{xy} \times Q_{31}^{xx})$$

$$/S/\ \text{REAL}\ (I_1^{xy} \times I_1^{xx}) + (Q_1^{xy} \times Q_1^{xx}) + (I_3^{xy} \times I_3^{xx}) + (Q_3^{xy} \times Q_3^{xx})$$

$$\ldots\ldots (I_{31}^{xy} \times I_{31}^{xx}) + (Q_{31}^{xy} \times Q_{31}^{xx})$$

(6) Store signs of REAL and IMAG

→ Save sign for quandrant test

→ Save sign for quadrant test

(7) Solve for V^{xy}

$$V^{xy} = \left(\frac{IMAG}{REAL}\right)$$

(8) Solve for ϕ^{xy}

$$\phi^{xy} = Tan^{-1} \quad (V^{xy})$$

(9) Correct ϕ^{xy} to $\overline{\phi^{xy}}$

By Correcting Tan^{-1} Quandrant Ambiguity using truth table.

Truth table

IMAG	REAL	Corrected $\overline{\phi^{xy}}$
+	+	$\phi^{xy} = \overline{\phi^{xy}}$
-	+	$\phi^{xy} - \pi = \overline{\phi^{xy}}$
-	-	$\pi - \phi^{xy} = \overline{\phi^{xy}}$
+	-	$2\pi - \phi^{xy} = \overline{\phi^{xy}}$

(10) Compute $\overline{\phi^{yx}}$ using same algorithm as shown in steps 2 through 9

(11) Elements that comprise the equation for the solution of $\overline{\phi^{yy}}$

$$\phi^{yy} \triangleq \text{Arg} \quad \Sigma A_i^{yy} \quad (A_{i-1}^{xx})^*$$

$$i = 2, 4, 6 \ldots\ldots N$$

(12) Substitution of mathematical operators and 'I' and 'Q' values for the I^{xx}, I^{yy}, Q^{xx}, and Q^{yy} terms

$$\overline{\phi^{yy}} \triangleq \text{Arg} \quad \Sigma (I^{yy} + jQ_i^{yy}) \times (I_{i-1}^{xx} - jQ_{i-1}^{xx})$$

$$i = 2, 4, 6, \ldots\ldots\ldots N$$

(13) Multiplication and collection of terms

$$(I_i^{yy} \times I_{i-1}^{xx}) + (jQ_i^{yy} \times I_{i-1}^{xx}) - (jQ_i^{yy} \times jQ_{i-1}^{xx}) - (I_i^{yy} \times jQ_{i-1}^{xx})$$

$$+ (Q_i^{yy} \times Q_{i-1}^{xx})$$

$$(I_i^{yy} \times I_{i-1}^{xx}) + (jQ_i^{yy} \times I_{i-1}^{xx}) + (Q_i^{yy} \times Q_{i-1}^{xx}) - (I_i^{yy} \times jQ_{i-1}^{xx})$$

(14) Sum the real and imaginary terms using all 16 of the even numbered Pulses (YY) and all 16 of the odd numbered Pulses (xx) using the following relationship:

$$/S/\ \text{IMAG} = (Q^{yy}_{2} \times I^{xx}_{1}) - (I^{yy}_{2} \times Q^{xx}_{1}) + (Q^{yy}_{4} \times I^{xx}_{3}) - (I^{yy}_{4} \times Q^{xx}_{3})$$

$$\ldots\ (Q^{xy}_{32} \times I^{xx}_{31}) - (I^{yy}_{32} \times Q^{xx}_{31})$$

$$/S/\ \text{REAL} = (I^{yy}_{2} \times I^{xx}_{1}) + (Q^{yy}_{2} \times Q^{xx}_{1}) + (I^{yy}_{4} \times I^{xx}_{3}) + (Q^{yy}_{4} \times Q^{xx}_{3})$$

$$\ldots\ (I^{yy}_{32} \times I^{xx}_{31}) + (Q^{xy}_{32} \times Q^{xx}_{31})$$

(15) Store signs for Real and Imaginary

Save sign for quadrant test

Save sign for quadrant test

(16) Solve for V^{yy}

$$V^{yy} = \left(\frac{IMAG}{REAL} \right)$$

(17) Solve for ϕ^{yy}

$$\phi^{yy} = \text{Tan}^{-1} (V^{yy})$$

(18) Correct ϕ^{yy} to $\overline{\phi^{yy}}$ by correcting Tan^{-1} quadrant ambiguity using truth table.

truth table

IMAG	REAL	Corrected $\overline{\phi^{yy}}$
+	+	$\phi^{yy} = \overline{\phi^{yy}}$
-	+	$\phi^{yy} - \pi = \overline{\phi^{yy}}$
-	-	$\pi - \phi^{yy} = \overline{\phi^{yy}}$
+	-	$2\pi - \phi^{yy} = \overline{\phi^{yy}}$

(19) The average phase, in units of radians, has been computed for

$\overline{\phi^{xy}}$, $\overline{\phi^{xx}}$, and $\overline{\phi^{yy}}$

(20) Computation of the mean values in the scattering matrix where the matrix elements are defined as:

$$S = \begin{bmatrix} \overline{S^{xx}} & \overline{S^{yx}}\, e^{j(\overline{\phi^{yx}} + \overline{\phi^{yy}} - \overline{\theta/2})} \\ \overline{S^{xy}}\, e^{j\,\overline{\phi^{xy}}} & \overline{S^{yy}}\, e^{j(\overline{\phi^{yy}} - \overline{\theta/2})} \end{bmatrix}$$

(21) Average the velocity values of fd_{yy} and fd_{xx} that were computed by the pulse pair processor.

$$\overline{fd} = \frac{fd_{yy} + fd_{xx}}{2}$$

(22) Convert average frequency $(\overline{fd})$ to angle in units of radians

$$\overline{\theta} = \frac{2\pi \times \overline{fd}}{PRF}$$

(23) Substituting values in matrix

$$S = \begin{bmatrix} \overline{S^{xx}} \angle 0 & \overline{S^{yx}} \angle \overline{\phi^{yx}} + \angle \overline{\phi^{yy}} - \angle \overline{\phi/2} \\ \overline{S^{xy}} \angle \overline{\phi^{xy}} & \overline{S^{yy}} \angle \overline{\phi^{yy}} - \angle \overline{\theta/2} \end{bmatrix}$$